

**ISTANBUL TECHNICAL UNIVERSITY ★ GRADUATE SCHOOL OF SCIENCE**  
**ENGINEERING AND TECHNOLOGY**

**SYNTHESIS AND CHARACTERIZATION OF COMPLEXES WITH A NEW  
ETHYLENEDIAMINE DERIVATIVE AND GROUP (IVB) METAL (Ti, Zr, Hf)  
SALTS**

**M.Sc. THESIS**

**İsmail Hakkı YÜCEL**

**Department of Chemistry**

**Chemistry Programme**

**JANUARY 2012**



**ISTANBUL TECHNICAL UNIVERSITY ★ GRADUATE SCHOOL OF SCIENCE**  
**ENGINEERING AND TECHNOLOGY**

**SYNTHESIS AND CHARACTERIZATION OF COMPLEXES WITH A NEW  
ETHYLENEDIAMINE DERIVATIVE AND GROUP (IVB) METAL (Ti, Zr, Hf)  
SALTS**

**M.Sc. THESIS**

**İsmail Hakkı YÜCEL**  
**(509071217)**

**Department of Chemistry**

**Chemistry Programme**

**Thesis Advisor: Prof. Dr. Ozan Sanlı ŞENTÜRK**

**JANUARY 2012**



**İSTANBUL TEKNİK ÜNİVERSİTESİ ★ FEN BİLİMLERİ ENSTİTÜSÜ**

**GRUP (IVB) METAL (Ti, Zr, Hf) TUZLARI VE YENİ BİR ETİLENDİAMİN  
TÜREVİ İLE KOMPLEKSLERİN SENTEZİ VE KARAKTERİZASYONU**

**YÜKSEK LİSANS TEZİ**

**İsmail Hakkı Yücel  
(509071217)**

**Kimya Anabilim Dalı**

**Kimya Programı**

**Tez Danışmanı: Prof. Dr. Ozan Sanlı ŞENTÜRK**

**OCAK 2012**



**İsmail Hakkı Yücel** a M.Sc. student of ITU Graduate School of Science Engineering and Technology student ID 509071217, successfully defended the thesis entitled “**SYNTHESIS AND CHARACTERIZATION OF COMPLEXES WITH A NEW ETHYLENEDIAMINE DERIVATIVE AND GROUP (IVB) METAL (Ti, Zr, Hf) SALTS**”, which he prepared after fulfilling the requirements specified in the associated legislations, before the jury whose signatures are below.

**Thesis Advisor :**      **Prof. Dr. Ozan Sanlı ŞENTÜRK**      .....

İstanbul Technical University

**Jury Members :**      **Prof. Dr. Ahmet GÜL**      .....

İstanbul Technical University

**Assoc. Prof. Dr. Ayşe ERÇAĞ**      .....

İstanbul University

**Date of Submission : 06 May 2011**

**Date of Defense : 05 January 2012**



*To my beloved family and fiancée,*



## **FOREWORD**

I would like to express my deep appreciation and thanks for my advisor Professor Ozan Sanlı ŞENTÜRK who gave me the opportunity to work on a laboratory equipped with all the technological accessories needed for air-sensitive chemistry, for his guidance, suggestions, discussions, encouragements and insight.

I would like to express my thanks to my laboratory partners Kerem KAYA, Fatma HAMURCU and Research Assistant Sibel KILIÇ for their support, help and friendship.

I would also thank to Research Assistants Ilgın NAR, Ufuk Saim GÜNAY and Volkan KUMBARACI for their help in discussions and writing my thesis.

January 2012

İsmail Hakkı YÜCEL  
(Chemist)



## TABLE OF CONTENTS

	<u>Page</u>
<b>FOREWORD</b> .....	<b>ix</b>
<b>TABLE OF CONTENTS</b> .....	<b>xi</b>
<b>ABBREVIATIONS</b> .....	<b>xiii</b>
<b>LIST OF FIGURES</b> .....	<b>xv</b>
<b>SUMMARY</b> .....	<b>xvii</b>
<b>ÖZET</b> .....	<b>xix</b>
<b>1. INTRODUCTION</b> .....	<b>1</b>
1.1 Polyolefins .....	1
1.2 Transition Metal Catalyst for Olefin .....	2
1.2.1 Phillips Catalysts .....	2
1.2.2 Ziegler-Natta Catalysts .....	3
1.2.3 Metallocene Catalysts .....	3
1.2.4 Post-Metallocene Catalysts .....	5
1.3 Single-Site Catalysts .....	6
1.4 Coordination or Insertion Polymerization .....	8
1.5 Activation of Catalysts .....	8
1.6 Termination of Polymerization .....	9
<b>2. GOAL OF THE THESIS</b> .....	<b>11</b>
<b>3. EXPERIMENTAL PART</b> .....	<b>13</b>
3.1 General.....	13
3.2 Synthesis of N,N-bis(perfluorophenyl)ethane-1,2-diamine, <b>(1)</b> .....	13
3.3 Synthesis of Tetrachloro N,N-bis(perfluorophenyl)ethane-1,2-diamine Titanium (IV), <b>(2)</b> .....	14
3.4 Synthesis of Tetrachloro N,N-bis(perfluorophenyl)ethane-1,2-diamine Zirconium (IV), <b>(3)</b> .....	15
3.5 Synthesis of Tetrachloro N,N-bis(perfluorophenyl)ethane-1,2-diamine Hafnium (IV), <b>(4)</b> .....	15
3.6 Synthesis of Disodium 1,2-diylbis((perfluorophenyl)amide)ethane, <b>(5)</b> .....	16
3.7 Synthesis of Dichloro 1,2-diylbis((perfluorophenyl)amide)ethane Zirconium (IV), <b>(6)</b> .....	16
3.8 Synthesis of Dichloro 1,2-diylbis((perfluorophenyl)amide)ethane Hafnium (IV), <b>(7)</b> .....	17
<b>4. RESULTS AND DISCUSSION</b> .....	<b>19</b>
4.1 Characterization of the Ligand .....	19
4.1.1 N,N-bis(perfluorophenyl)ethane-1,2-diamine, <b>(1)</b> .....	19
4.2 Characterization of the Metal Complexes .....	20
4.2.1 Via Direct Reaction .....	20
4.2.1.1 Tetrachloro N,N-bis(perfluorophenyl)ethane-1,2-diamine Titanium (IV), <b>(2)</b> .....	21

4.2.1.2 Tetrachloro N,N-bis(perfluorophenyl)ethane-1,2-diamine Zirconium (IV), (3) .....	22
4.2.1.3 Tetrachloro N,N-bis(perfluorophenyl)ethane-1,2-diamine Hafnium (IV), (4).....	23
4.2.2 Via Disodium Salt.....	24
4.2.2.1 Disodium 1,2-diylbis((perfluorophenyl)amide)ethane, (5) .....	24
4.2.2.2 Dichloro 1,2-diylbis((perfluorophenyl)amide)ethane Zirconium (IV), (6) .....	25
4.2.2.3 Dichloro 1,2-diylbis((perfluorophenyl)amide)ethane Hafnium (IV), (7) .....	26
<b>5. CONCLUSION .....</b>	<b>29</b>
<b>REFERENCES .....</b>	<b>31</b>
<b>APPENDICES .....</b>	<b>35</b>
APPENDIX A.1 GC-MS Data .....	35
APPENDIX A.2 <sup>1</sup> H-NMR Spectra .....	36
APPENDIX A.1 <sup>13</sup> C-NMR Spectra.....	40
APPENDIX A.1 <sup>19</sup> F-NMR Spectra .....	41
APPENDIX A.1 FT-IR Spectra.....	45
<b>CURRICULUM VITAE.....</b>	<b>49</b>

## ABBREVIATIONS

<b>ATR</b>	: Attenuated Total Reflectance
<b>CH<sub>2</sub>Cl<sub>2</sub></b>	: Dichloromethane or Methylenechloride
<b>Et<sub>2</sub>O</b>	: Diethylether
<b>FT</b>	: Fourier transform
<b>g</b>	: Gram(s)
<b>HDPE</b>	: High Density Polyethylene
<b>Hf</b>	: Hafnium
<b>HPLC</b>	: High Performance Liquid Chromatography
<b>Hz</b>	: Hertz
<b>IR</b>	: Infrared
<b>LLDPE</b>	: Linear Low Density Polyethylene
<b>M</b>	: Metal
<b>MAO</b>	: Methylaluminoxane
<b>mmol</b>	: Milimol (10 <sup>-3</sup> mol)
<b>NMR</b>	: Nuclear Magnetic Resonance
<b>Ppm</b>	: Particules per million
<b>THF</b>	: Tetrahydrofuran
<b>Ti</b>	: Titanium
<b>Vacuo</b>	: Vacuum
<b>Zr</b>	: Zirconium



## LIST OF FIGURES

	<u>Page</u>
<b>Figure 1.1</b> : Examples of Polyolefin Application . . . . .	1
<b>Figure 1.2</b> : Monometallic Ziegler-Natta Polymerization Mechanism. . . . .	2
<b>Figure 1.3</b> : Chromium based Phillips Catalysts. . . . .	3
<b>Figure 1.4</b> : Structures of different type of Metallocene Catalysts. . . . .	4
<b>Figure 1.5</b> : Example of a Post-Metallocene Catalyst. . . . .	5
<b>Figure 1.6</b> : Example of Post-Metallocene Single Site Catalysts. . . . .	7
<b>Figure 1.7</b> : Coordination of a Monomer (Mo) to a Metal (M) . . . . .	8
<b>Figure 1.8</b> : Activation of a Metallocene Precatalyst by MAO . . . . .	8
<b>Figure 1.9</b> : Activation of a Post-Metallocene Precatalyst by borate cocatalyst . . . . .	9
<b>Figure 1.10</b> : Beta-Hydrogen Elimination . . . . .	9
<b>Figure 1.11</b> : Beta-Hydrogen Transfer to Monomer . . . . .	10
<b>Figure 4.1</b> : FT-IR spectra of <b>PFA and (1)</b> . . . . .	20
<b>Figure 4.2</b> : <sup>1</sup> H-NMR spectra of <b>PFA and (1)</b> . . . . .	20
<b>Figure 4.3</b> : FT-IR spectra of <b>(1) and (2)</b> . . . . .	22
<b>Figure 4.4</b> : <sup>1</sup> H-NMR spectra of <b>(1) and (2)</b> . . . . .	22
<b>Figure 4.5</b> : <sup>1</sup> H-NMR spectra of <b>(1) and (3)</b> . . . . .	23
<b>Figure 4.6</b> : <sup>1</sup> H-NMR spectra of <b>(1) and (4)</b> . . . . .	24
<b>Figure 4.7</b> : <sup>1</sup> H-NMR spectra of <b>(1) and (5)</b> . . . . .	25
<b>Figure 4.8</b> : FT-IR Spectra of <b>(1) and (6)</b> . . . . .	26
<b>Figure 4.9</b> : <sup>1</sup> H-NMR spectra of <b>(6)</b> . . . . .	26
<b>Figure 4.10</b> : FT-IR spectra of <b>(1) and (7)</b> . . . . .	27
<b>Figure 4.11</b> : <sup>1</sup> H-NMR spectra of <b>(7)</b> . . . . .	28
<b>Figure A.1</b> : Gas Chromatogram of <b>(1)</b> . . . . .	35
<b>Figure A.2</b> : Mass spectrum of <b>(1)</b> . . . . .	36
<b>Figure A.3</b> : <sup>1</sup> H-NMR spectrum of <b>PFA</b> . . . . .	37
<b>Figure A.4</b> : <sup>1</sup> H-NMR spectrum of <b>(1)</b> . . . . .	37
<b>Figure A.5</b> : <sup>1</sup> H-NMR spectrum of <b>(2)</b> . . . . .	38
<b>Figure A.6</b> : <sup>1</sup> H-NMR spectrum of <b>(3)</b> . . . . .	38
<b>Figure A.7</b> : <sup>1</sup> H-NMR spectrum of <b>(4)</b> . . . . .	39
<b>Figure A.8</b> : <sup>1</sup> H-NMR spectrum of <b>(5)</b> . . . . .	39
<b>Figure A.9</b> : <sup>1</sup> H-NMR spectrum of <b>(6)</b> . . . . .	40
<b>Figure A.10</b> : <sup>1</sup> H-NMR spectrum of <b>(7)</b> . . . . .	40
<b>Figure A.11</b> : <sup>13</sup> C-NMR spectrum of <b>PFA</b> . . . . .	40
<b>Figure A.12</b> : <sup>13</sup> C-NMR spectrum of <b>(1)</b> . . . . .	41
<b>Figure A.13</b> : <sup>19</sup> F-NMR spectrum of <b>PFA</b> . . . . .	41
<b>Figure A.14</b> : <sup>19</sup> F-NMR spectrum of <b>(1)</b> . . . . .	42
<b>Figure A.15</b> : <sup>19</sup> F-NMR spectrum of <b>(2)</b> . . . . .	42
<b>Figure A.16</b> : <sup>19</sup> F-NMR spectrum of <b>(3)</b> . . . . .	43
<b>Figure A.17</b> : <sup>19</sup> F-NMR spectrum of <b>(4)</b> . . . . .	43
<b>Figure A.18</b> : <sup>19</sup> F-NMR spectrum of <b>(6)</b> . . . . .	44

<b>Figure A.19</b> : $^{19}\text{F}$ -NMR spectrum of <b>(7)</b> .....	44
<b>Figure A.20</b> : FT-IR spectrum of <b>PFA</b> ...	45
<b>Figure A.21</b> : FT-IR spectrum of <b>(1)</b> .....	45
<b>Figure A.22</b> : FT-IR spectrum of <b>(2)</b> ...	46
<b>Figure A.23</b> : FT-IR spectrum of <b>(3)</b> .....	46
<b>Figure A.24</b> : FT-IR spectrum of <b>(6)</b> ...	47
<b>Figure A.25</b> : FT-IR spectrum of <b>(7)</b> .....	47

# SYNTHESIS AND CHARACTERIZATION OF COMPLEXES WITH A NEW ETHYLENEDIAMINE DERIVATIVE AND GROUP (IVB) METAL (Ti, Zr, Hf) SALTS

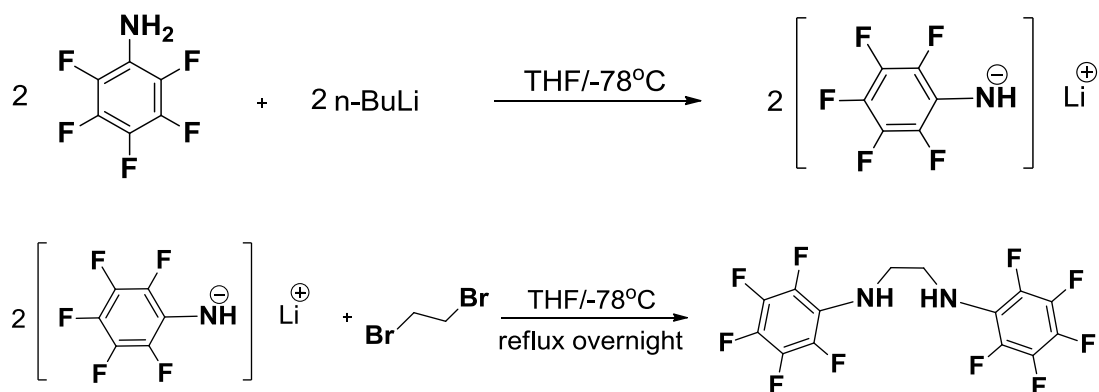
## SUMMARY

The design and synthesis of new transition-metal catalyst precursors is a very important subject that can provide high catalytic activity with low cocatalyst-to-catalyst precursor (pre-catalyst) ratios and allows unprecedented control over the polymer microstructure, producing new polymers with improved polymer properties.

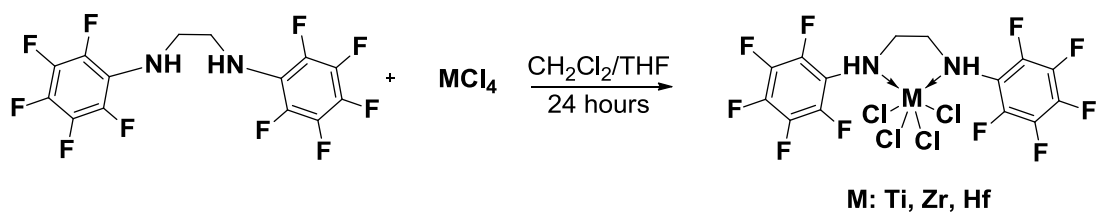
In this aspect homogeneous single-site olefin polymerization catalysts have developed rapidly in the last few decades with the group 4 cyclopentadienyl compounds. For example, although the catalyst precursor  $\text{Cp}_2\text{ZrCl}_2$  will polymerize ethylene with high activity, the homopolymerization of  $\alpha$ -olefins is relatively slow. In contrast Cp-amide derivatives readily incorporate  $\alpha$ -olefins.

Complexes of group (IVB) chelating diamine ligands serve as highly active precursors for the living polymerization of  $\alpha$ -olefins. This success of complexes that are produced from nitrogen-based ligand systems, prompted investigations on the polymerization chemistry of group (IVB) chelating diamide complexes. The substituents bound to the amido nitrogens may influence the reactivity of the catalyst by inducing electronic and steric effects in the close vicinity of the metal centre. Also electron withdrawing groups are expected to increase the electrophilicity of the metal centre thereby enhancing its tendency to interact with olefins.

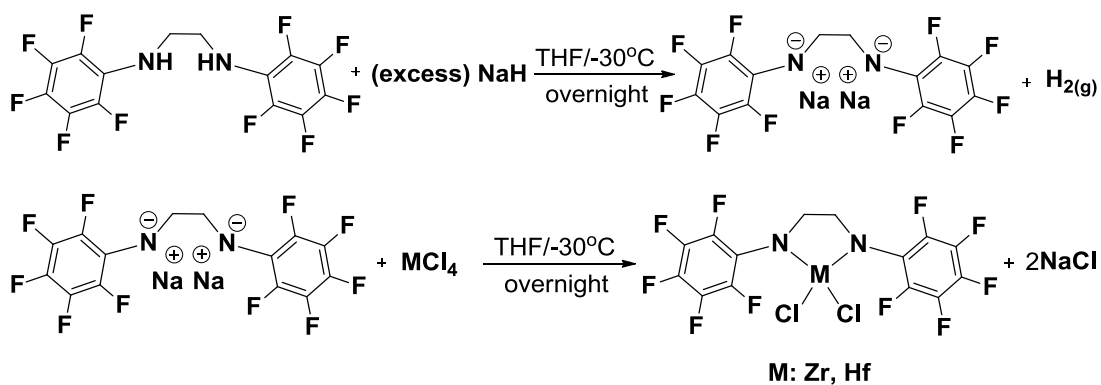
In this study, a new nitrogen-based fluorinated chelating diamine ligand was synthesized by in-situ deprotonation of pentafluoroaniline with  $n\text{-BuLi}$  in THF and the addition of 1,2-dibromoethane and then stirring under reflux overnight. New nitrogen-based fluorinated chelating diamine ligand is expected to form a 5-membered chelate ring by the reaction with group (IVB) metal salts.



$\text{MCl}_4\text{L}^{\wedge}\text{L}$  type of complexes were obtained by the direct reactions of new diamine ligand with  $\text{MCl}_4$  (M: Ti, Zr, Hf) in organic solvent such as THF or  $\text{CH}_2\text{Cl}_2$  at room temperature under inert atmosphere.



$MCl_2L^+L^-$  type of complexes were obtained by the reaction of  $MCl_4$  (M: Zr, Hf) with the disodium salt of new diamine ligand which was produced by the reaction between diamine ligand and excess sodium hydride (NaH).



## GRUP (IVB) METAL (Ti, Zr, Hf) TUZLARI VE YENİ BİR ETİLENDİAMİN TÜREVİ İLE KOMPLEKSLERİNİN SENTEZİ VE KARAKTERİZASYONU

### ÖZET

Poliolefinler, etilen, propilen ya da sitiren gibi basit alken monomerlerinden üretilen polimerlerdir. Aynı zamanda polialkenler olarak da isimlendirilmektedirler. Poliolefinler en yaygın biçimde kullanılan sentetik polimerlerdir. Dünya çapındaki tüm polimer üretiminin ağırlıkça %90'ını ve tüm polimer eşyaların yaklaşık %50'sini poliolefinler oluşturmaktadır. Değişik uygulama alanına ve değişik özelliklere sahip yüzlerce poliolefin sınıfı mevcuttur. Değişik özellikler gösteren ve değişik uygulama alanlarına sahip bu poliolefinlerin üretiminde yeni geçiş metali katalizörler kullanılmaktadır.

Yeni geçiş metali katalizörlerinin tasarlanması ve sentezlenmesi yüksek katalitik aktivite gösterebilen ve düşük katalizör / kokatalizör oranına ihtiyaç duyan katalizörlerin elde edilebilmesi açısından büyük önem taşımaktadır. Bu katalizörler sayesinde polimerin mikroyapısı üzerinde kontrol sağlanıp gelişmiş özelliklere sahip polimerler elde edilebilir. Bu bağlamda homojen olefin polimerizasyon katalizörleri çok hızlı bir gelişim göstermiştir.

Olefin polimerizasyon katalizörlerinde aranan özellikler şu şekilde sıralanabilir;

- Katalizör yüksek olefin katabilme özelliğine sahip olmalı,
- Katalizör polimerizasyon için cis- pozisyonda iki uygun alan buldurmalı,
- Katalizör genel polimerizasyon koşulları altında kararlı olmalı,
- Geri bağda hacimli süstitüentler barındırmalı,
- Aktif merkez elektronca fakir olmalıdır.

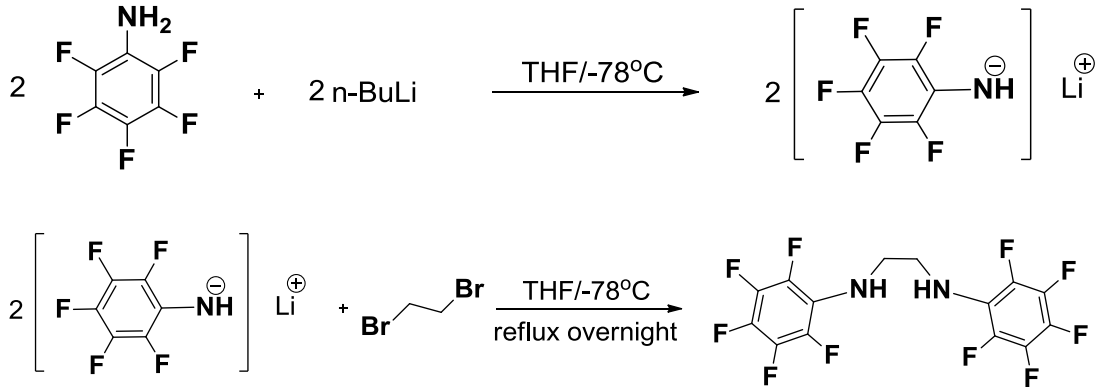
Son yıllarda azot heteroatomu içeren ligandlar olefin polimerizasyonunda başarıyla kullanılmaya başlanmıştır. Örneğin;  $Cp_2ZrCl_2$ , etileni çok hızlı bir şekilde polimerleştirmesine rağmen,  $\alpha$ -olefinlerin homopolimerizasyonu göreceli olarak yavaştır. Buna karşın, Cp-amin türevleri,  $\alpha$ -olefinleri kolayca polimerleştirebilmektedir.

Şelat diamin türevleri içeren kompleksler olefin polimerizasyonunda yüksek katalitik aktivite göstermektedirler. Azot heteroatomlu ligand sistemlerinden üretilen bu komplekslerin olefin polimerizasyonundaki başarısı, son yıllarda bu konu ile ilgili çalışmaların yoğunluk kazanmasına yol açmıştır.

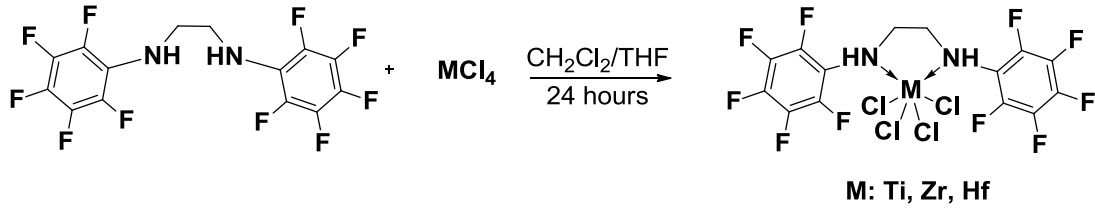
Grup (IVB) metallerinin şelat yapıcı dianyonik diamido ligandlarıyla oluşturdukları kompleksler büyük ilgi çekmiştir. Şelat yapıcı dianyonik diamino ligandlarına bağlı olan süstitüentler elektronik ve sterik özellikler açısından oldukça önem taşımaktadırlar. Buna bağlı olarak en çok tercih edilen gruplar aril ya da trialkilsilil gruplarıdır. Aril ya da trialkilsilil gruplarına bağlı atom ya da gruplar da elektronik özellikler açısından önemlidir. Elektron çekici bir grup varlığında metal merkezin elektrofiliği artar. Bu sayede metal merkezin aktivitesi de artmış olur.

Sentezlenen kompleksler genellikle MAO, borat türevleri ya da anilinyum tuzları içeren bir ko-katalizör yardımı ile aktive edilerek olefin polimerizasyonunda başlatıcı olarak kullanılırlar. Ko-katalizörler, metal üzerinde genellikle katyonik, bir koordinasyon boşluğu oluştururlar ve olefin monomeri bu koordinasyon boşluğuna yerleşerek metale koordine olur. Metal üzerinde bulunan diğer alkil grubu olefin monomerinin ucuna göç eder ve bu sırada ayrılmış olduğu yerde yeni bir koordinasyon boşluğu oluşturur ve aynı işlem tekrarlanır. Katalizör / ko-katalizör oranı komplekse göre farklılık göstermekle birlikte genellikle 1:1000 dir. Ko-katalizör kullanımı maliyet açısından büyük bir dezavantaj oluştursa da yüksek aktivite sağlaması açısından oldukça önem teşkil etmektedir.

Bu çalışmada, elektron çekici özelliğe sahip yeni bir florlu diamin ligandı, pentafloroanilinün n-BuLi ile THF içerisinde deprotonasyonu, 1,2-dibromoetan ilavesi ve ardından geri soğutucu altında karıştırılmasıyla sentezlenmiştir. Sentezlenen yeni florlu diamin ligandının grup (IVB) metal tuzları ile reaksiyonları sonucu ile 5 üyeli bir şelat halkası oluşturabileceği öngörülmüştür.

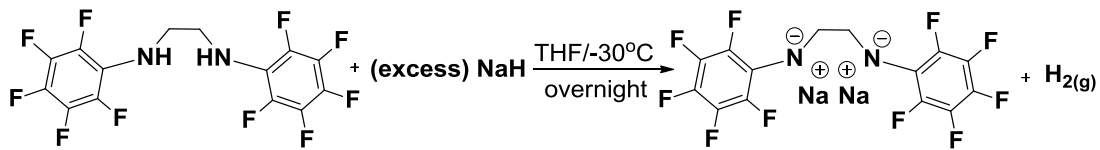


Yeni florlu diamin ligandının  $\text{MCl}_4$  (M: Ti, Zr, Hf) ile inert atmosferde, oda sıcaklığında THF veya  $\text{CH}_2\text{Cl}_2$  içerisinde direkt tepkimesi sonucu dört klor atomu içeren  $\text{MCl}_4\text{L}^{\wedge}$  L tipi kompleksler elde edilmiştir.

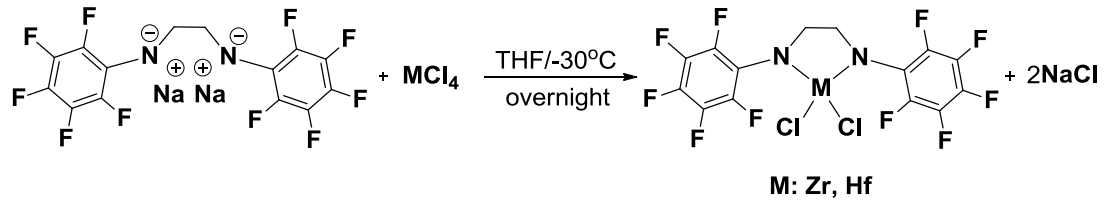


$\text{MCl}_4\text{L}^{\wedge}$  L tipi komplekslerde metal (Ti, Zr, Hf) atomlarına, azot atomları üzerinde bulunan non-bonding elektronları üzerinden koordinasyon söz konusudur.  $\text{MCl}_4\text{L}^{\wedge}$  L tipi kompleksler 12 elektron sistemine uymaktadır ve elektronca fakirdir.

Yeni florlu diamin ligandının, THF içerisinde aşırı miktarda sodyum hidrür (NaH) ile tepkimeye sokulmasıyla diamin ligandının disodyum tuzu elde edilmiştir.



Diamin ligandından elde edilen disodyum tuzlarının THF içerisinde  $\text{MCl}_4$  (M: Zr, Hf) ile tepkimesi sonucu  $\text{MCl}_4\text{L}^{\wedge}$  L tipi komplekslerden farklı olarak iki klor atomu içeren  $\text{MCl}_2\text{L}^{\wedge}$  L tipi kompleksler elde edilmiştir.



$MCl_2L^+$  L tipi kompleksler, azot atomları ile metal (Zr, Hf) atomları arasında sigma bağları bulundururlar. 8 elektrona sahip elektronca fakir komplekslerdir ve oldukça reaktiflerdir.

$MCl_2L^+$  L tipi kompleksler  $\alpha$ -olefinlerin polimerizasyonunda kullanılacak aday katalizörler olabilirler.



## 1. INTRODUCTION

### 1.1 Polyolefins

Polyolefins are polymers made from simple alkenes as monomers like ethylene, propylene or styrene. An equivalent term is polyalkene, although most of the people prefer the term polyolefin. They are the most widely used synthetic polymers. They represent approximately 50% of all commodity polymers and 90% by weight of the global polymer production. There are hundreds of polyolefins grades available with different properties and different applications [1].

Polyolefinic materials, as represented by polyethylenes (PEs), polypropylenes (PPs), ethylene/  $\alpha$  -olefin amorphous copolymers, and ethylene/propylene/diene elastomers (EPDMs) are not only huge molecules, but they are also manufactured and consumed in huge amounts. Their worldwide consumption exceeded 100 million tons in the year 2008, and this is predicted to increase at an average annual growth rate of more than 5% [2].

There is an incredible variety of properties for polyolefins. Polyolefins from ultra-rigid thermosets stiffer than steel to high-performance elastomers. Moreover, these materials are cost-effective and possess good chemical inertness and recyclability. The applications include plastic shopping bags, food packages, shampoo and detergent bottles, containers, storage boxes, disposable diapers, bullet-proof vests and automotive interior and exterior parts (e.g., instrument panels, glass run channels, door trim) [1] (Figure 1.1). Thus, they have become indispensable materials for modern living and directly impact our daily lives in countless beneficial ways. But looking at the chemical compositions polyolefins are so few; polyethylenes, polypropylenes and some copolymers of polyethylenes with an  $\alpha$ -olefin. The key reason behind this contradiction is the molecular control of the polymerization process by the modern transition based metal catalysts. Transition metal catalysts makes possible to produce olefins with precisely defined properties by controlling the molecular weight, molecular weight distribution and the tacticity [3].



**Figure 1.1:** Examples of polyolefin application.

## 1.2 Transition Metal Catalysts for Olefin Polymerization

In the past, the term “Ziegler–Natta catalysts” was used as a general expression that describes a variety of catalysts based on transition metal compounds and capable of polymerizing and copolymerizing alkenes and dienes. However, the development of numerous new catalysts for alkene polymerization in the last 20 years called for separation of all transition metal-based polymerization catalysts into several groups [4].

### 1.2.1 Ziegler-Natta Catalysts

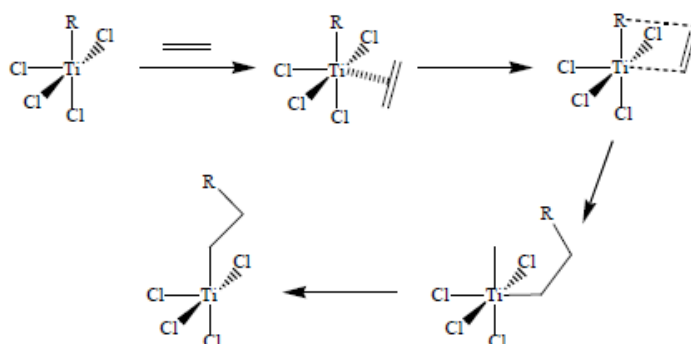


**Figure 1.2:** Monometallic Ziegler-Natta polymerization mechanism.

The first group, which includes mostly titanium and vanadium-based catalysts, has retained the name “Ziegler–Natta catalysts.” These catalysts are named after Karl Ziegler (Germany) and Giulio Natta (Italy). In the early 1950s, these chemists discovered the first catalytically active compositions for alkene polymerization, determined principles of their action, and investigated the structures and properties of polymers produced with the catalysts. The monumental contributions of Ziegler and Natta received universal recognition and these scientists were jointly awarded the Nobel Prize in chemistry in 1963. Ziegler–Natta catalysts have been used in the commercial manufacture of various polymeric materials since 1956 [5].

Natta received universal recognition and these scientists were jointly awarded the Nobel Prize in chemistry in 1963. Ziegler–Natta catalysts have been used in the commercial manufacture of various polymeric materials since 1956 [5].

### 1.2.2 Phillips Catalysts

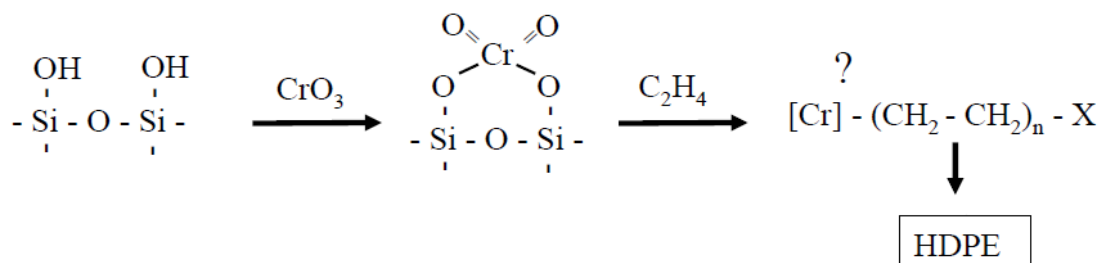


**Figure 1.3:** Chromium based Phillips catalysts.

The second group constitutes chromium-based catalysts. Historically, chromium oxide catalysts were the first transition metal catalysts used for alkene polymerization; J. P. Hogan and R. L. Banks (USA) discovered them in the early 1950s. Phillips Petroleum Company extensively used these catalysts for the polymerization of ethylene to high molecular, highly crystalline ethylene homopolymers. Later, researchers at Phillips Petroleum Company have found that the same type of catalyst, after modification, is suitable for the polymerization of other alkenes and for alkene copolymerization reactions [5].

### 1.2.3 Metallocene Catalysts

The third catalyst group are commonly called “metallocene polymerization catalysts.” D. Breslow (USA) and G. Natta discovered first metallocene catalysts for alkene polymerization soon after the original discovery of the Ziegler–Natta catalysts. The early metallocene catalysts had relatively low activity and were regarded as most suitable for academic research [6]. However, German scientists W. Kaminsky and H. Sinn in 1976 discovered a new class of metallocene catalyst systems that exhibit extremely high activity [5]. A large number of metallocene complexes can be used in Kaminsky–Sinn catalysts. They usually belong to the following classes:

- Bis(cyclopentadienyl) complexes  $\text{Cp}_2\text{MX}_2$ , where M is Titanium, Zirconium, or Hafnium, and X are halogen atoms, H, or small alkyl groups. The cyclopentadienyl groups can carry various alkyl substituents.

- Bis-metallocene complexes in which one or both ligands are indenyl groups  $C_9H_7$ , tetrahydroindenyl groups,  $C_9H_{11}$ , or fluorenyl groups,  $C_{13}H_9$ .
- Bridged metallocene complexes with cyclopentadienyl, indenyl, tetrahydroindenyl, and fluorenyl ligands. The bridges connect two cyclopentadienyl rings. The most frequently used bridges are  $-CH_2-CH_2-$ ,  $WSiMe_2$ ,  $WMe_2$ ,  $WSiPh_2$ , and  $-CHPh-CHPh-$  [5].

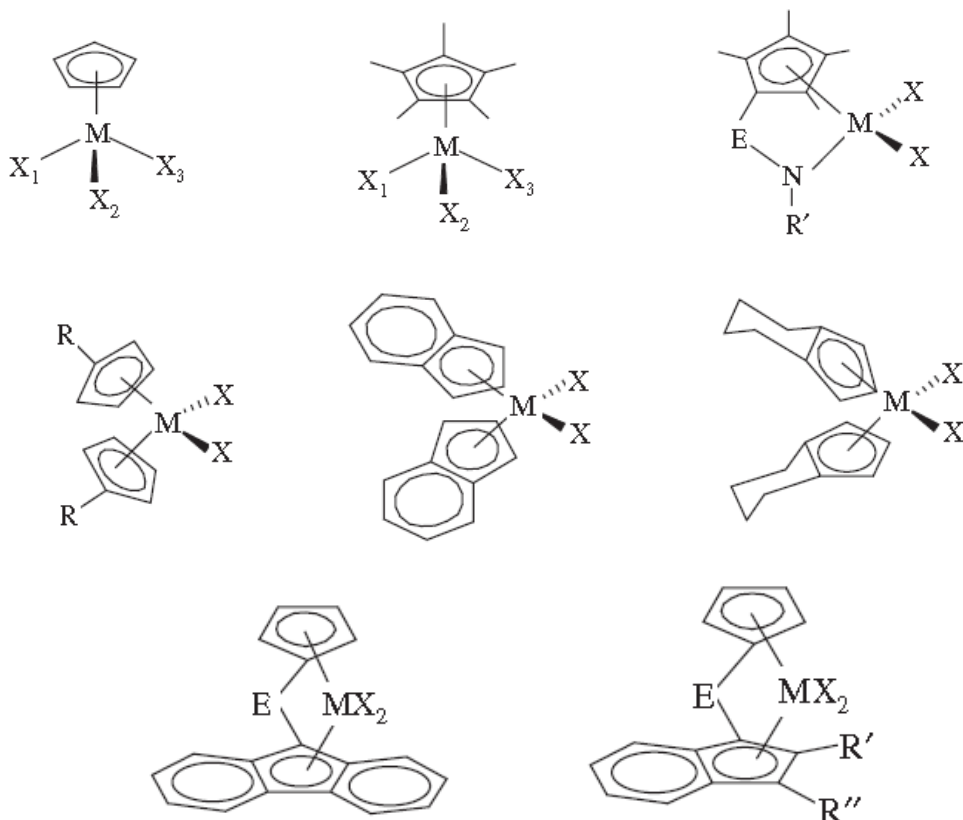


**Figure 1.4:** Structures of different type of metallocene catalysts.

The structures of these metallocene complexes are shown in Figure 1.4. Among metallocene complexes of this type, zirconium complexes are usually preferred because of their high activity. When polymerization reactions with Kaminsky–Sinn catalysts are carried out in solution, either in an aromatic or in an aliphatic solvent, the  $[MAO]:[Zr]$  ratio is usually high, 1,000–2,000, although much lower ratios are employed under commercial conditions. Kaminsky–Sinn catalysts, when used for ethylene polymerization in toluene solutions at sufficiently high  $[Al]:[Zr]$  ratios, exhibit exceptionally high activity. Many commercial polymerization processes require preparation of supported Kaminsky–Sinn catalysts. Nowadays, two types of metallocene complexes are widely used as components of catalyst systems. The first

type of the metallocene complex contains two cyclopentadienyl rings attached to a transition metal atom (usually Zr, Ti, rarely Hf) and the second type contains one cyclopentadienyl ring. Both types of metallocene complexes were the subjects of an enormous volume of research, both in academia and in industry. These catalysts and their subsequent modifications presently compete with Ziegler–Natta catalysts for many applications [6].

In spite of the success of metallocene catalysts in polymerization reactions, they also exhibit some disadvantages. These catalysts need a large amount of MAO or expensive fluorinated borate activators to obtain adequate polymerization activity, which causes concern over the high cost of metallocene catalysts and the high ash ( $\text{Al}_2\text{O}_3$ ) content of the product polymers. Consequently, there is a great need to develop new catalyst systems that can provide high catalytic activity with no need for a large amount of expensive cocatalysts [3].

#### 1.2.4 Post-Metallocene Catalysts

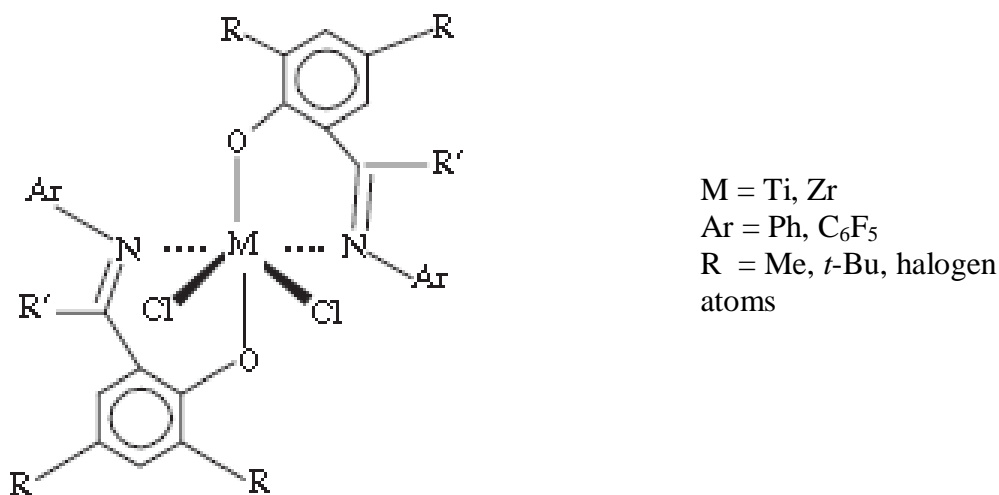


**Figure 1.5:** Example of a Post-Metallocene catalyst.

The fourth group includes polymerization catalysts based on hydrocarbon-soluble non-metallocene transition metal complexes. M. Brookhart (USA) in 1995 discovered the first catalysts of this type. In the past several years this field underwent a rapid development and now encompasses well-defined complexes of many early-period and late-period transition metals in the Periodic Table [6]. At the present time, the development of homogeneous catalyst systems based on non-metallocene complexes of various transition metals is the leading research area in the field of alkene polymerization catalysis. A large variety of multidentate complexes of

early- and late-period transition metals are being explored. Some of these catalysts are relatively stable in a polar environment. They also provide the best route to the synthesis of alkene copolymers with polar vinyl compounds. The family of non-metallocene homogeneous catalysts utilizes a variety of complexes of various metals, ranging from  $d^0$  metals (Sc) to lanthanoid and actinoid metals, and a large variety of monodentate, bidentate, and multidentate ligands containing oxygen, nitrogen, phosphorus, and sulfur as metal-coordinating atoms. The complexes are usually isolated and are well characterized by the single crystal X-ray method. They are transformed into polymerization catalysts using the same cocatalysts as those in metallocene catalysis, MAO or ion-forming activators under mild conditions [5].

### 1.3 Single-Site Catalysts

The definition of a single type of active center in a catalytic polymerization reaction can be formulated on the basis of its kinetic and stereochemical properties. Active centers of a single type have the following common characteristics:

- 1) The value of the propagation rate constant in a polymerization reaction of a particular alkene, as well as the rate constants of all chain transfer reactions, is the same for all the centers. These kinetic features lead to a particular type of the molecular weight distribution of any polymer produced with uniform active centers.
- 2) The stereospecificity of all the centers of a given type (represented, e.g., by the probability of steric errors in homopolymer chains) is the same. This characteristic leads to a very narrow stereoregularity distribution of alkene homopolymers.
- 3) In copolymerization reactions of two alkenes, relative reactivities of the alkenes are the same for all the centers of a given type. This characteristic leads to a narrow compositional distribution of alkene copolymers [2].

While the multi-sited heterogeneous Ziegler–Natta catalysts represented by  $MgCl_2$  - supported  $TiCl_4$  catalysts currently dominate the market, molecular catalysts (single-site catalysts) represented by group 4 metallocene catalysts and post-metallocene catalysts are gaining an increasing presence in the market. Benefits of the single-site catalysts include the ability to produce polymers with controlled molecular weight,

specific tacticity, improved molecular weight distribution, and better comonomer distribution and content [8]. With these advantages, the single site catalysts have allowed the preparation of a wide variety of new or differentiated polyolefinic materials, which include high-performance LLDPE (linear low-density polyethylene), polyolefinic elastomers, cyclic olefin copolymers, ethylene/styrene copolymers, highly isotactic and syndiotactic PPs (iPPs and sPPs), and highly syndiotactipolystyrenes (sPSs) [7].

Additionally, recently emerging non-metallocene or so-called “post-metallocene” single-site catalysts (Figure 1.3) have enabled synthesizing distinctive polymers such as hyperbranched PE’s, ethylene/polar monomer copolymers and higher  $\alpha$  -olefin-based block copolymers, which are difficult or virtually impossible to produce using group 4 metallocene catalysts. Moreover, the post-metallocene catalysts have provided systematic opportunities to study the mechanisms of the initiation, propagation, and termination steps of coordination (insertion) polymerization and the mechanisms of stereospecific polymerization [8]. This has significantly contributed to advances in the rational design of catalysts for the controlled copolymerization of olefinic monomers. Altogether, the development of high performance post-metallocene catalysts has made a dramatic impact on polymer synthesis and catalysis chemistry. There is thus great interest in the development of new non-metallocene catalysts for olefin polymerization with a view to achieving unique catalysis and distinctive polymer synthesis [9].

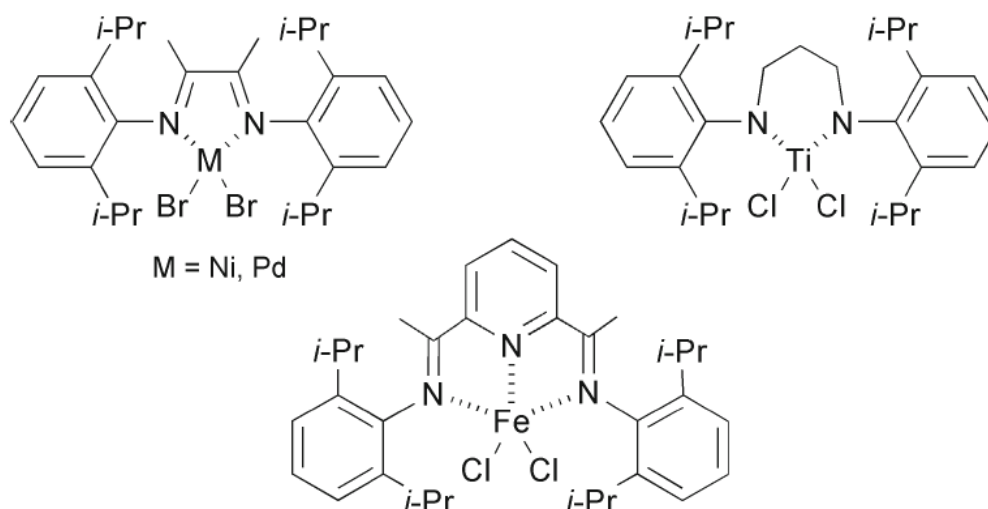


**Figure 1.6:** Examples of post-metallocene single site catalysts.

## 1.4 Coordination or Insertion Polymerisation

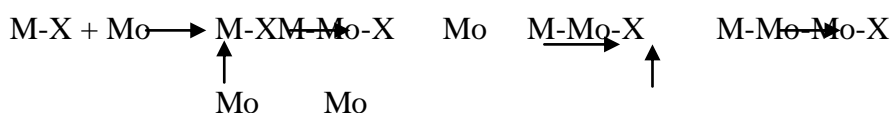


**Figure 1.7:** Coordination of a monomer (Mo) to a metal (M).

Polymerisation carried out in the presence of a coordination catalyst is referred to as “coordination polymerisation” or “insertion polymerisation”, when each step involves the complexation of monomer before its enchainment at the active site of the catalyst. The active site in each coordination catalyst comprises the metal atom (M) surrounded with ligands’ one of which (X) forms a covalent active bond (M-X) with this metal atom. This implies that the growing polymer chain is covalently bound to the metal atom. A characteristic feature of coordination polymerisation is the mutual activation of the reacting bonds of both the monomer (Mo) and the active site (M-X) through the complexation of the monomer with the metal atom at this site, which results in the cleavage of these bonds in the concerted reaction [10].

The coordination step proposed in many polymerisation systems with coordination catalysts has not been fully established. Thus, the more general term ‘insertion polymerisation’ has been used for these polymerisations systems to imply a hindered propagation site and to avoid implying the unproven coordination aspect.

## 1.5 Activation of Catalysts

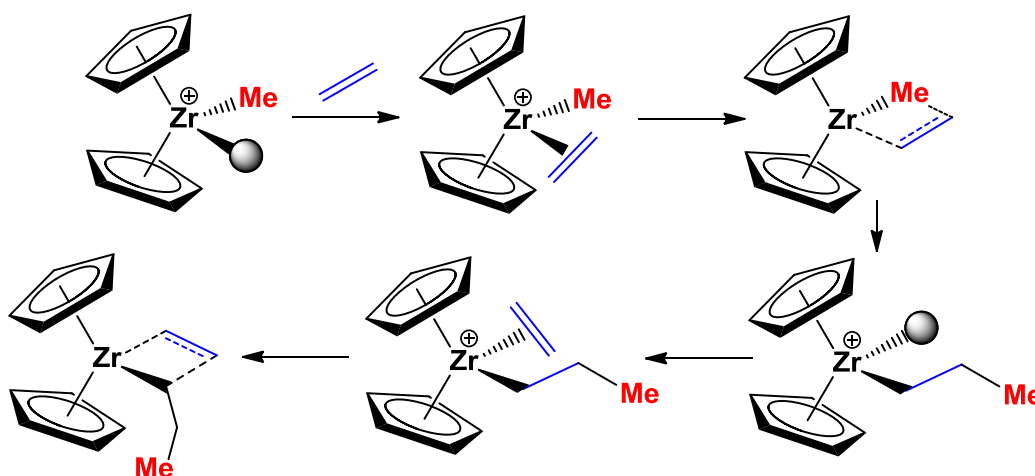


**Figure 1.8:** Activation of a metallocene pre-catalyst by MAO.

The activation of polymerization catalysts based on coordination complexes consists of generating an equilibrium concentration of a coordinatively unsaturated species,

usually cationic, that contains a reactive metal-alkyl bond and is capable of binding an olefin in such a manner that transfer of the alkyl ligand to the monomer can occur. MAO is the most widely employed activator in the industry of group 4 polymerization catalysts. Methylalumoxane activates metallocene catalysts by virtue of Lewis acidic sites on some of the complex structures present in MAO [11].

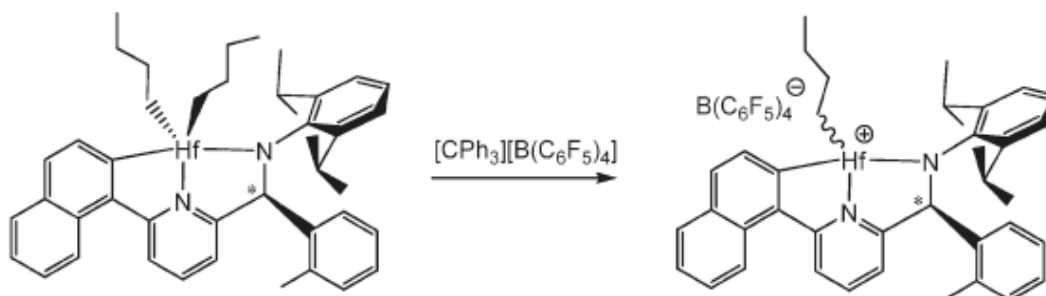


**Figure 1.9:** Activation of a Post-Metallocene precatalyst by borate cocatalyst.

This activation can also be achieved by reacting metal dialkyl complexes, usually the metal dimethyls  $\text{LnMMe}_2$  (M: Ti, Zr, Hf) (Ln:Ligand) with suitable Lewis acids such as  $\text{B}(\text{C}_6\text{F}_5)_3$  and triphenylmethyl (“trityl”) salts of noncoordinating anions, or Brønsted acids capable of generating weakly coordinating counteranions. Among the last class of activators, anilinium salts such as  $[\text{HNR}_2\text{Ph}][\text{B}(\text{C}_6\text{F}_5)_4]$  (R: Me, Et) have been widely used [11].

## 1.6 Termination of Polymerization

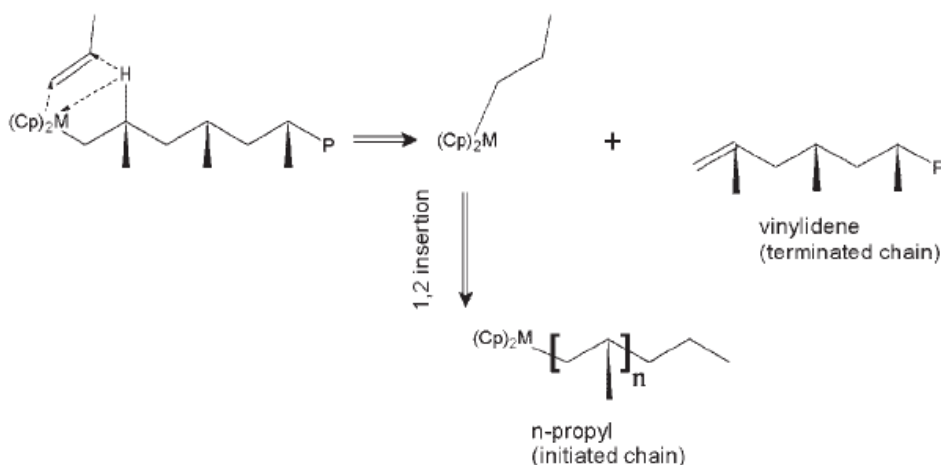


**Figure 1.10:** Beta-Hydrogen elimination.

One of the most important properties of a polymer is its average chain length. For metal-catalyzed olefin polymerization, the degree of polymerization is determined by

the ratio between the rate of propagation and those of all possible chain termination mechanisms. There are many potential chain termination reactions. The most important ones are hydrogen elimination (BHE) and hydrogen transfer to monomer (BHT) [12].

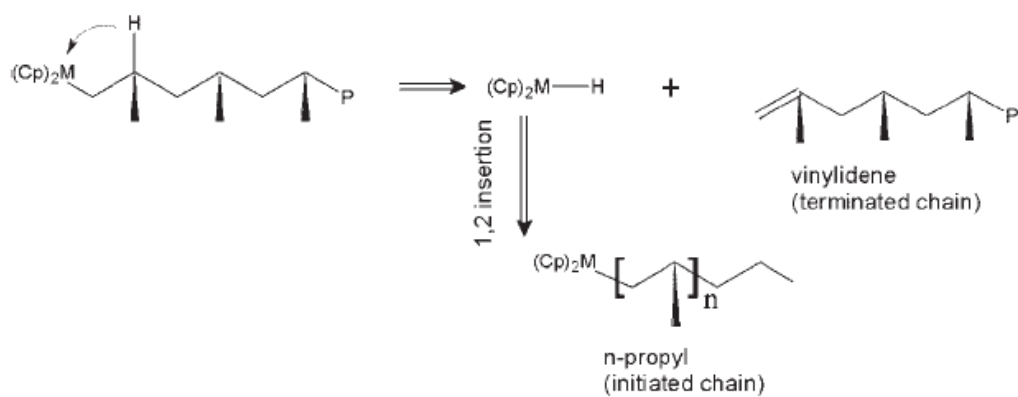


**Figure 1.11:** Beta-Hydrogen transfer to monomer.

## 2. GOAL OF THE THESIS

The general requirements for a highly active polymerization precatalyst are:

- A catalyst must have high olefin-insertion ability.
- A catalyst must have two available *cis*-located sites for polymerization.
- A catalyst must be stable enough under usual polymerization conditions [13].

Bulky substituents in the ligand are generally considered to be necessary for olefin polymerization catalysts [14]. Electron-withdrawing substituents are routinely incorporated to enhance the electrophilicity of the metal center, giving improved activities [15]. In comparison with the dihalide complexes only a few of the tri or tetrahalide non-metallocene precursors were found to be active for olefin polymerization. One of the reasons is probably that the space of the central metal in the tri or tetrachloride complex is more open than in the similar dichloride species because the chlorine atom is small, influencing the chain-transfer process of polymerization [16, 17]. Electron-withdrawing, fluorinated aryl groups are expected to provide highly electrophilic, reactive metal centers [18]. The presence of fluorine interaction with the central metal ion is sometimes possible which renders the complex more active [19]. In addition to that, highly fluorinated group 4 metal complexes exhibit increased robustness over the non-fluorinated analogues and can survive even at high temperatures (over 100°C) which could be necessary for a good catalytic activity [15].

Considering all the necessary properties of an efficient olefin polymerization catalyst that explained above, we aimed to synthesize and characterize a new chelating diamine ligand and its titanium, zirconium and hafnium complexes in this thesis. These complexes can serve as highly active precursors in the polymerization of olefins [13-25].

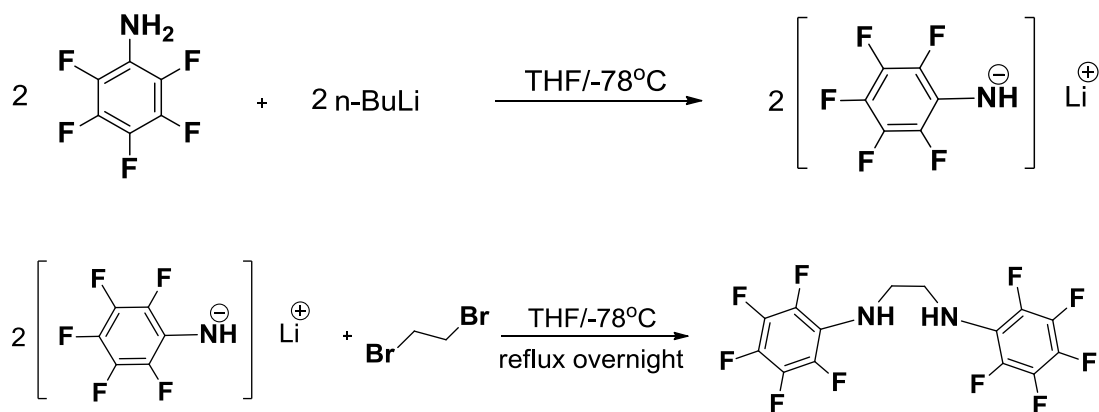


### 3. EXPERIMENTAL PART

#### 3.1 General

All the manipulations for the titanium, zirconium and hafnium complexes were carried out in an inert (Nitrogen) atmosphere using standard Schlenk techniques or in an Innovative Glovebox with O<sub>2</sub> level below 5 ppm and H<sub>2</sub>O level below 1 ppm. All the solvents used were HPLC grade solvents distilled prior to use in an Innovative Solvent Purification System with special molecular sieves and catalysts (activated alumina) which eliminates trace amount of water. Melting point was measured on a Buchi B540 instrument. Thermo EK-90 immersion cooler is used for the experiments which are carried out in low temperatures. GC-Mass analysis was taken on a Thermo Finnigan Trace DSQ GC spectrometer. <sup>1</sup>H-NMR spectra used in the characterization of products were recorded on Varian 500 MHz and Bruker 250 MHz AC Aspect 3000 spectrometer with tetramethylsilane as internal reference. <sup>13</sup>C and <sup>19</sup>F NMR spectra used in the characterization of compounds were recorded in Varian 500 MHz spectrometer. Infrared Spectra of ligand and complexes were taken in a Perkin Elmer Spectrum-One FT-IR instrument with ATR accessory. All the chemicals were used as they were purchased.

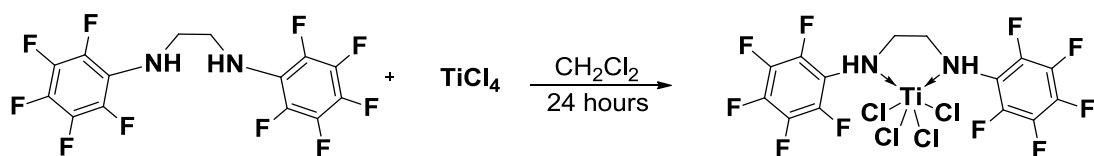
#### 3.2 Synthesis of N,N-bis(perfluorophenyl)ethane-1,2-diamine, (1):



5.82 g pentafluoroaniline (19.8 mmol) was weighed into a Schlenk flask and dissolved in 20 mL of dry THF under nitrogen. The solution was cooled to -78 °C by

using immersion cooler in acetone bath and 8 mL of 2.5 M *n*-BuLi (20 mmol) was added dropwise. The dark red solution was stirred for 10 minutes, and 0.866 mL of 1,2-dibromoethane (10.00 mmol) was added dropwise over 15 minutes period. The solution was allowed to warm to room temperature over 1 hour period and then was refluxed overnight. The THF solvent was removed under reduced pressure, and the residue was redissolved in diethylether. Water was carefully added, and the dark red organic phase was separated and dried over anhydrous MgSO<sub>4</sub>. After filtration, the ether solution was reduced in volume approximately to 2 mL and transferred to a short-path distillation apparatus. The remaining ether was removed, and the residue was heated at 120 °C (10<sup>-1</sup> mmHg) to distill off all remaining pentafluoroaniline. The black tarry residue was extracted with diethyl ether and taken to dryness. Recrystallization is repeated from hot hexane yielded dark orange product. Yield: 27%. Mp: 58,5-60 °C. IR (ATR) :  $\nu(\text{N-H})$  3438 cm<sup>-1</sup>,  $\nu(\text{C-H})$  2981-2849 cm<sup>-1</sup>,  $\delta(\text{N-H})_{\text{def}}$  1656 cm<sup>-1</sup>,  $\nu(\text{C=C})$  1514 cm<sup>-1</sup>,  $\nu(\text{C-N})_{\text{aryl}}$  1326 cm<sup>-1</sup>,  $\nu(\text{C-N})_{\text{alkyl}}$  1242 cm<sup>-1</sup>. <sup>1</sup>H-NMR (500MHz, CDCl<sub>3</sub>) :  $\delta$  3.52 (s, 4H, CH<sub>2</sub>),  $\delta$  3.77 (s, 2H, NH). <sup>13</sup>C-NMR{<sup>1</sup>H} (125MHz, CDCl<sub>3</sub>) :  $\delta$  46.55 (t, CH<sub>2</sub>),  $\delta$  123.25 (t, *quat*-arylC),  $\delta$  133.09 (dm, *p*-arylC),  $\delta$  137.28 (dm, *o*-arylC),  $\delta$  139.17 (dm, *m*-arylC). <sup>19</sup>F-NMR{<sup>1</sup>H} (470MHz, CDCl<sub>3</sub>) :  $\delta$  -159.12 (d, *o*-arylF),  $\delta$  -163.86 (dt, *m*-arylF),  $\delta$  -170.20 (tt, *p*-arylF). MS found (calcd) : M<sup>+</sup> 391.8 (392.04).

### 3.3 Synthesis of Tetrachloro N,N-bis(perfluorophenyl)ethane-1,2-diamine Titanium (IV), (2):

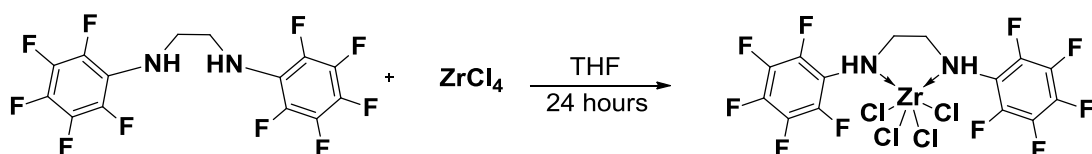


10 mL methylenechloride solution of 0.392g (1 mmol) N,N-bis(perfluorophenyl)ethane-1,2-diamine was added to a 5 mL methylenechloride solution of 0.1 mL (1 mmol) TiCl<sub>4</sub> in glove-box at room temperature. The color of reaction mixture turned immediately from yellow to red and left out stirring overnight in a Schlenk flask. After that the reaction mixture was filtered through celite 545 pad and solvent was removed under vacuo. The residue was washed with *n*-hexane and dried. The red titanium complex was obtained. Yield: 35%. IR (ATR) :  $\nu(\text{N-H})$  3215 cm<sup>-1</sup>,  $\nu(\text{C-H})$  3037-2903 cm<sup>-1</sup>,  $\delta(\text{N-H})_{\text{def}}$  1658 cm<sup>-1</sup>,  $\nu(\text{C=C})$  1520 cm<sup>-1</sup>,

$\nu(\text{C-N})_{\text{alkyl}}$  1241.58  $\text{cm}^{-1}$ .  $^1\text{H-NMR}$  (500MHz,  $\text{CDCl}_3$ ) :  $\delta$  3.54 (s, 4H,  $\text{CH}_2$ ),  $\delta$  4.05 (s, 2H, NH).  $^{19}\text{F-NMR}\{^1\text{H}\}$  (470MHz,  $\text{CDCl}_3$ ) :  $\delta$  -158.96 (*o*-arylF),  $\delta$  -163.76 (*m*-arylF),  $\delta$  -170.02 (*p*-arylF).

### 3.4 Synthesis of Tetrachloro N,N-bis(perfluorophenyl)ethane-1,2-diamine

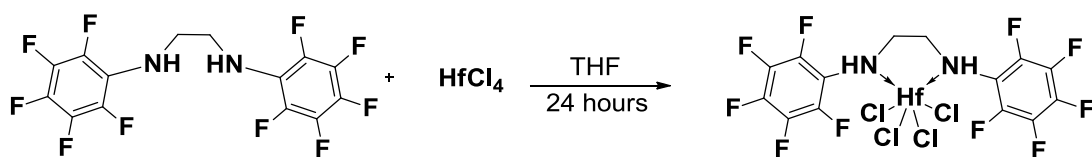
#### Zirconium (IV), (3):



5 mL THF solution of 0.156 g (0.4 mmol) N,N-bis(perfluorophenyl)ethane-1,2-diamine was added dropwise over 15 minutes period to a 10 mL THF solution 0.0932 g (0.4 mmol)  $\text{ZrCl}_4$  at room temperature in glove-box. The color of reaction mixture became pale yellow and left out stirring overnight in a Schlenk flask. After that the reaction mixture was filtered through celite 545 pad and the solvent was removed under vacuo. The residue was washed with n-hexane and dried. The yellow zirconium complex was obtained. Yield: 36%.  $\nu(\text{N-H})$  3232  $\text{cm}^{-1}$ ,  $\nu(\text{C-H})$  2903-2980  $\text{cm}^{-1}$ ,  $\delta(\text{N-H})_{\text{def}}$  1656  $\text{cm}^{-1}$ ,  $\nu(\text{C=C})$  1514  $\text{cm}^{-1}$ ,  $\nu(\text{C-N})_{\text{alkyl}}$  1242  $\text{cm}^{-1}$ .  $^1\text{H-NMR}$  (500MHz,  $\text{CDCl}_3$ ) :  $\delta$  3.54 (s, 4H,  $\text{CH}_2$ ),  $\delta$  4.21 (s, 2H, NH).  $^{19}\text{F-NMR}\{^1\text{H}\}$  (470MHz,  $\text{CDCl}_3$ ) :  $\delta$  -158.53 (*o*-arylF),  $\delta$  -163.53 (*m*-arylF),  $\delta$  -169.26 (*p*-arylF).

### 3.5 Synthesis of Tetrachloro N,N-bis(perfluorophenyl)ethane-1,2-diamine

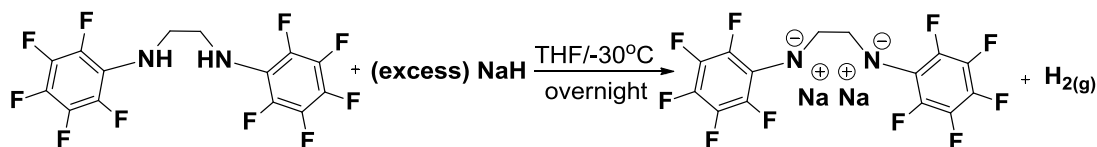
#### Hafnium (IV), (4):



5 mL THF solution of 0.156 g (0.4 mmol) N,N-bis(perfluorophenyl)ethane-1,2-diamine was added dropwise over 10 minutes period to a 7 mL THF solution of 0.1281 g (0.4 mmol)  $\text{HfCl}_4$  at room temperature in glove-box. The color of reaction mixture became pale yellow and left out stirring overnight in a Schlenk flask. After that the reaction mixture was filtered through celite 545 pad and the solvent was removed under vacuo. The residue was washed with n-hexane and dried. The yellow hafnium complex was obtained. Yield: 39%.  $^1\text{H-NMR}$  (500MHz,  $\text{CDCl}_3$ ) :  $\delta$  3.59 (s,

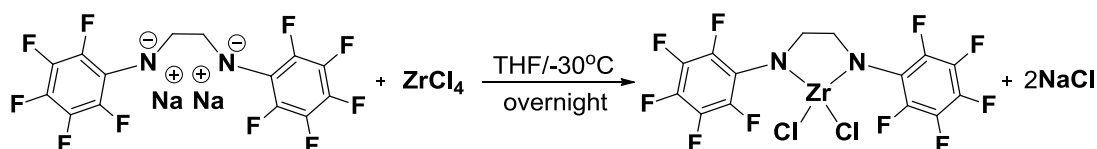
4H, CH<sub>2</sub>), δ 4.81 (s, 2H, NH). <sup>19</sup>F-NMR{<sup>1</sup>H} (470MHz, CDCl<sub>3</sub>) : δ -157.30 (*o*-arylF), δ -162.80 (*m*-arylF), δ -167.14 (*p*-arylF).

### 3.6 Synthesis of Disodium 1,2-diylbis((perfluorophenyl)amide)ethane, (5):



10 mL THF solution of 0.784 g (2 mmol) N,N-bis(perfluorophenyl)ethane-1,2-diamine and 10 mL THF suspension of 0,144 g (6 mmol) NaH were cooled to -30°C in freezer inside the glove-box for four hours. After four hours, THF suspension of NaH was added dropwise to THF solution of N,N-bis(perfluorophenyl)ethane-1,2-diamine. The color of the reaction mixture was turned to dark green from dark orange and H<sub>2</sub> evolution was observed. The reaction mixture left out stirring overnight. After that the reaction mixture was filtered through celite 545 pad for eliminating the remaining NaH and the solvent was removed under vacuo. The dark green disodium salt of ligand was obtained after washing with dry n-hexane. <sup>1</sup>H-NMR (250MHz, CDCl<sub>3</sub>) : δ 3.72 (s, 4H, CH<sub>2</sub>).

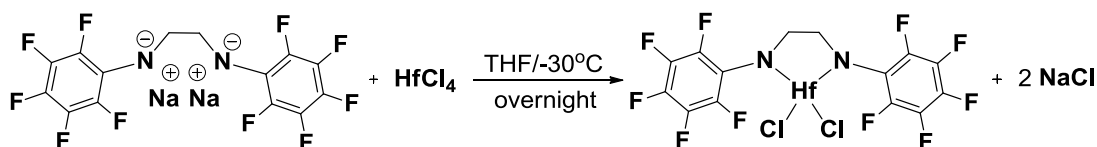
### 3.7 Synthesis of Dichloro 1,2-diylbis((perfluorophenyl)amide)ethane Zirconium (IV), (6):



0.1165 g (0,5 mmol) ZrCl<sub>4</sub> was dissolved in 10 mL of THF and cooled to -30°C in the freezer inside of the glove-box. The chilled THF solution of 0.218 g (0,5 mmol) disodium 1,2-diylbis((perfluorophenyl)amide)ethane salt was added dropwise to ZrCl<sub>4</sub>(THF)<sub>2</sub> solution in 10 minutes in the glove-box. After the addition of a few drops of disodium 1,2-diylbis((perfluorophenyl)amide)ethane salt, the color of the reaction mixture changed from colorless to pale red. The reaction mixture was filtered through celite 545 pad for eliminating NaCl. After the filtration, the solvent was removed under vacuo and pale red residue was obtained after washing twice with 5 mL n-hexane. Yield: 37%. IR (ATR) : ν(C-H) 2955-2874 cm<sup>-1</sup>, ν(C=C) 1491

$\text{cm}^{-1}$ ,  $\nu(\text{C-N})_{\text{aryl}}$  1365  $\text{cm}^{-1}$ ,  $\nu(\text{C-N})_{\text{alkyl}}$  1246  $\text{cm}^{-1}$ .  $^1\text{H-NMR}$  (500MHz,  $\text{CDCl}_3$ ) :  $\delta$  4.35 (s, 4H,  $\text{CH}_2$ ).  $^{19}\text{F-NMR}\{^1\text{H}\}$  (470MHz,  $\text{CDCl}_3$ ) :  $\delta$  -148.93 (*o*-arylF),  $\delta$  -153.08 (*m*-arylF),  $\delta$  -163.37 (*p*-arylF).

### 3.8 Synthesis of Dichloro 1,2-diylbis((perfluorophenyl)amide)ethane Hafnium (IV), (7):



0.160 g (0,5 mmol)  $\text{HfCl}_4$  was dissolved in 10 mL of THF and cooled to  $-30^\circ\text{C}$  in freezer inside of the glove-box. The chilled THF solution of 0.218 g (0,5 mmol) disodium 1,2-diylbis((perfluorophenyl)amide)ethane salt was added dropwise to  $\text{HfCl}_4(\text{THF})_2$  solution in 10 minutes in the glove-box. After the addition of a few drops of disodium 1,2-diylbis((perfluorophenyl)amide)ethane salt, the color of the reaction mixture changed from colorless to pale red. The reaction mixture was filtered through celite 545 pad for eliminating  $\text{NaCl}$ . After the filtration, solvent was removed under vacuo. After the filtration, the solvent was removed under vacuo and pale red residue was obtained after washing twice with 5 mL n-hexane. Yield: 40%. IR (ATR) :  $\nu(\text{C-H})$  2944-2874  $\text{cm}^{-1}$ ,  $\nu(\text{C=C})$  1491  $\text{cm}^{-1}$ ,  $\nu(\text{C-N})_{\text{aryl}}$  1365  $\text{cm}^{-1}$ ,  $\nu(\text{C-N})_{\text{alkyl}}$  1246  $\text{cm}^{-1}$ .  $^1\text{H-NMR}$  (250MHz,  $\text{CDCl}_3$ ) :  $\delta$  4.39 (s, 4H,  $\text{CH}_2$ ).  $^{19}\text{F-NMR}\{^1\text{H}\}$  (470MHz,  $\text{CDCl}_3$ ) :  $\delta$  -149.02 (*o*-arylF),  $\delta$  -153.13 (*m*-arylF),  $\delta$  -163.29 (*p*-arylF).



## 4. RESULTS AND DISCUSSION

### 4.1 Characterization of the Ligand

N,N-bis(perfluorophenyl)ethane-1,2-diamine was prepared by reaction of 1,2-dibromoethane with the aniline anion which was obtained by in-situ deprotonation of pentafluoroaniline with n-BuLi. FT-IR,  $^1\text{H-NMR}$ ,  $^{13}\text{C-NMR}$ ,  $^{19}\text{F-NMR}$  and GC-MS methods were used in the characterization of the N,N-bis(perfluorophenyl)ethane-1,2-diamine. All the spectroscopic evidences proved the formation of N,N-bis(perfluorophenyl)ethane-1,2-diamine.

#### 4.1.1 N,N-bis(perfluorophenyl)ethane-1,2-diamine, (**1**):

According to FT-IR datum of **pentafluoroaniline (PFA)**, asymm. and symm.  $\text{ArF-NH}_2$  stretching bands appear at 3513 and 3417  $\text{cm}^{-1}$ . By the formation of **1**,  $\text{ArFNH-CH}_2\text{-CH}_2\text{-NHArF}$ , one of the  $\text{NH}_2$  stretching bands disappeared and the other shifted to 3438  $\text{cm}^{-1}$  in comparison to the FT-IR spectrum of **PFA**. New  $\text{CH}$  stretching bands of **1**,  $\text{ArFNH-CH}_2\text{-CH}_2\text{-NHArF}$ , were observed between 2981 – 2849  $\text{cm}^{-1}$  and a new  $\text{CN}$ ,  $\text{ArFHN-CH}_2\text{-H}_2\text{C-NHArF}$ , aliphatic stretching band appeared at 1242  $\text{cm}^{-1}$ . The FT-IR spectrum of **1** was shown in **Fig. 4.1** and **Fig. A.21**. According to  $^1\text{H-NMR}$  spectrum of **1**,  $\text{NH}$  protons,  $\text{ArFNH-CH}_2\text{-CH}_2\text{-NHArF}$ , observed at 3.77 ppm and a new signal that belongs to  $\text{CH}_2$  protons,  $\text{ArFNH-CH}_2\text{-CH}_2\text{-NHArF}$ , were appeared at 3.52 ppm. The integration ratio of protons is accorded with the proposed structure. The  $^1\text{H-NMR}$  spectrum of **1** was shown in **Fig. 4.2** and **Fig. A.4**. According to  $^{13}\text{C-NMR}$  spectrum of **1**,  $\text{Ar}$  carbons,  $\text{ArFNH-CH}_2\text{-CH}_2\text{-NHArF}$ , were observed between 123 – 139 ppm and a new signal that belongs to  $\text{CH}_2$  carbons,  $\text{ArFNH-CH}_2\text{-CH}_2\text{-NHArF}$ , was appeared at 46.59 ppm. The  $^{13}\text{C-NMR}$  spectrum of **1** was shown in **Fig. A.12**. According to  $^{19}\text{F-NMR}$  spectrum of **1**, the signals belong to  $\text{ArF}$ ,  $\text{ArFNH-CH}_2\text{-CH}_2\text{-NHArF}$ , shifted 3-5 ppm downfield in comparison to **PFA**. The  $^{19}\text{F-NMR}$  spectrum of **1** was shown in **Fig. A.14**. The gas chromatogram of **1** shows one single peak that proved the compound was pure. The Gas chromatogram of **1** was shown in

**Fig. A.1.** Mass spectrum showed a peak at 391,8 which was assigned as molecular ion. The Mass spectrum of **1** was shown in **Fig. A.2**.

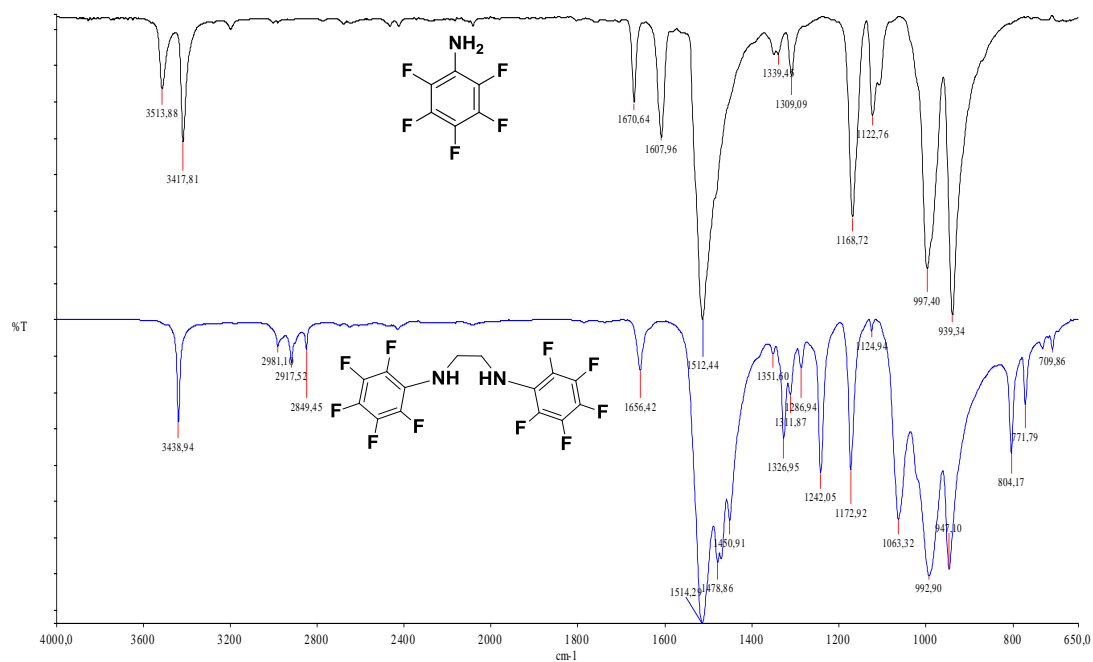


**Figure 4.1:** FT-IR spectra of **PFA** and **1**.

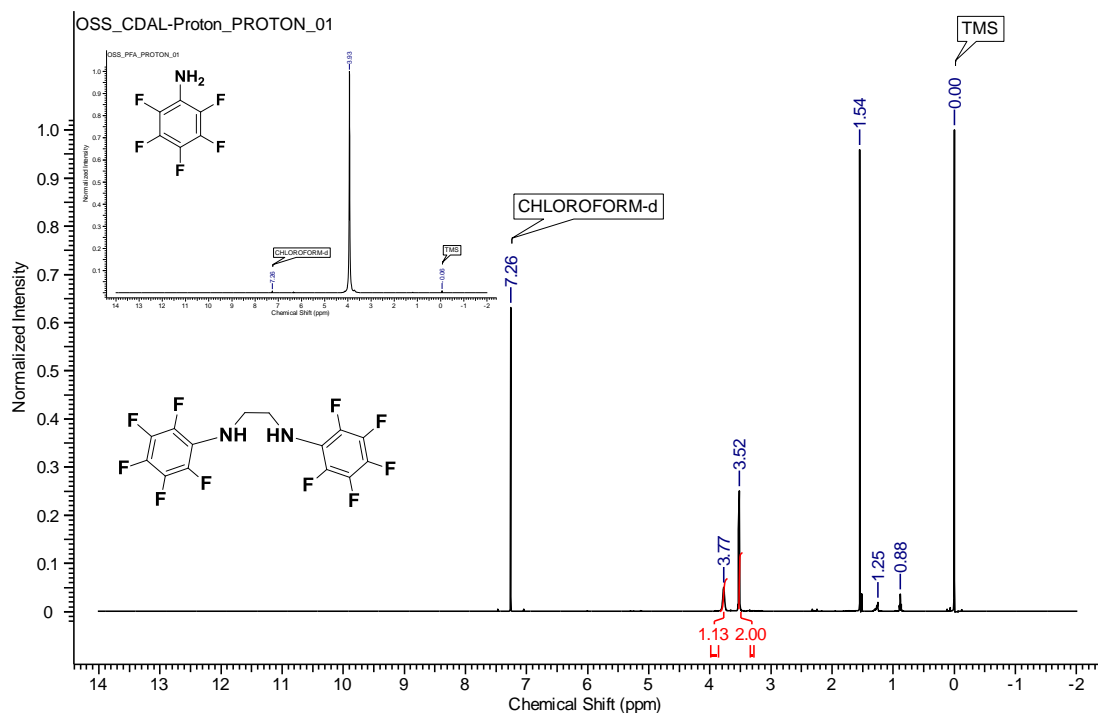


**Figure 4.2:**  $^1\text{H-NMR}$  spectra of **PFA** and **1**.

## 4.2 Characterization of the Metal Complexes

$MCl_4L^{\wedge}L$  type of complexes were prepared by the direct reactions of a new diamine ligand ( $L^{\wedge}L$ : N,N-bis(perfluorophenyl)ethane-1,2-diamine) with  $MCl_4$  (M: Ti, Zr, Hf) in organic solvent such as THF or  $CH_2Cl_2$  at room temperature under inert atmosphere.  $MCl_2L^{\wedge}L$  type of complexes were prepared by the reaction of  $MCl_4$  (M: Zr, Hf) with the disodium salt  $Na_2(ArFN-CH_2-CH_2-NArF)$  of new diamine ligand which was produced by the reaction between diamine ligand and excess sodium hydride (NaH).

### 4.2.1 Via Direct Reaction between $[MCl_4]$ (M: Ti, Zr, Hf) and N,N-bis(perfluorophenyl)ethane-1,2-diamine, $L^{\wedge}L$ .

$MCl_4L^{\wedge}L$  type of complexes were prepared by the direct reaction between  $MCl_4$  (M: Ti, Zr, Hf) and N,N-bis(perfluorophenyl)ethane-1,2-diamine in  $CH_2Cl_2$  or THF. These complexes were characterized by FT-IR,  $^1H$ -NMR and  $^{19}F$ -NMR methods.

#### 4.2.1.1 Tetrachloro N,N-bis(perfluorophenyl)ethane-1,2-diamine Titanium (IV), (2):

According to FT-IR datum of **2**,  $NH$  stretching band,  $ArFNH-CH_2-CH_2-NHArF$ , was shifted to  $3215\text{ cm}^{-1}$  due to coordination via lone-pair electrons of nitrogen atoms to titanium. The FT-IR spectrum of **2** was shown in **Fig. 4.3** and **Fig. A.22**. According to  $^1H$ -NMR spectrum of **2**,  $CH_2$  protons,  $ArFNH-CH_2-CH_2-NHArF$ , shifted 0.02 ppm to downfield and were observed at 3.54 ppm.  $NH$  protons,  $ArFNH-CH_2-CH_2-NHArF$ , shifted 0.3 ppm to downfield and were observed at 4.05 ppm which was reasonable due to the coordination of nitrogen atoms to titanium. The  $^1H$ -NMR spectrum of **2** was shown in **Fig. 4.4** and **Fig. A.5**. According to  $^{19}F$ -NMR spectrum of **2**,  $ArF$  signals,  $ArFNH-CH_2-CH_2-NHArF$ , shifted slightly. The  $^{19}F$ -NMR spectrum of **2** was shown in **Fig. A.15**.

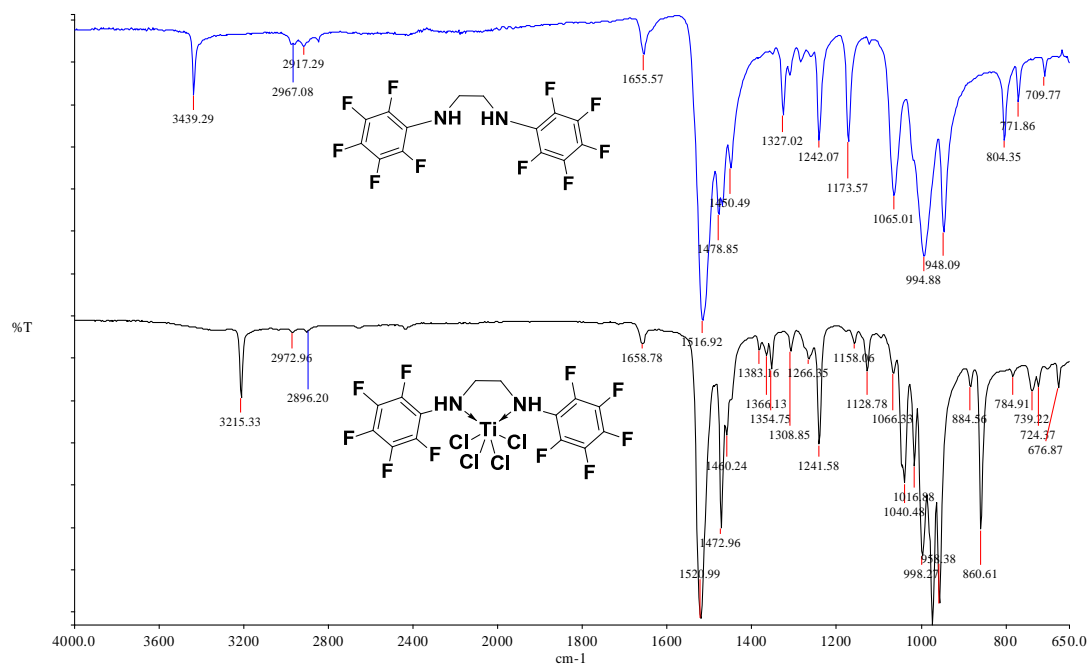


Figure 4.3: FT-IR spectra of **1** and **2**.

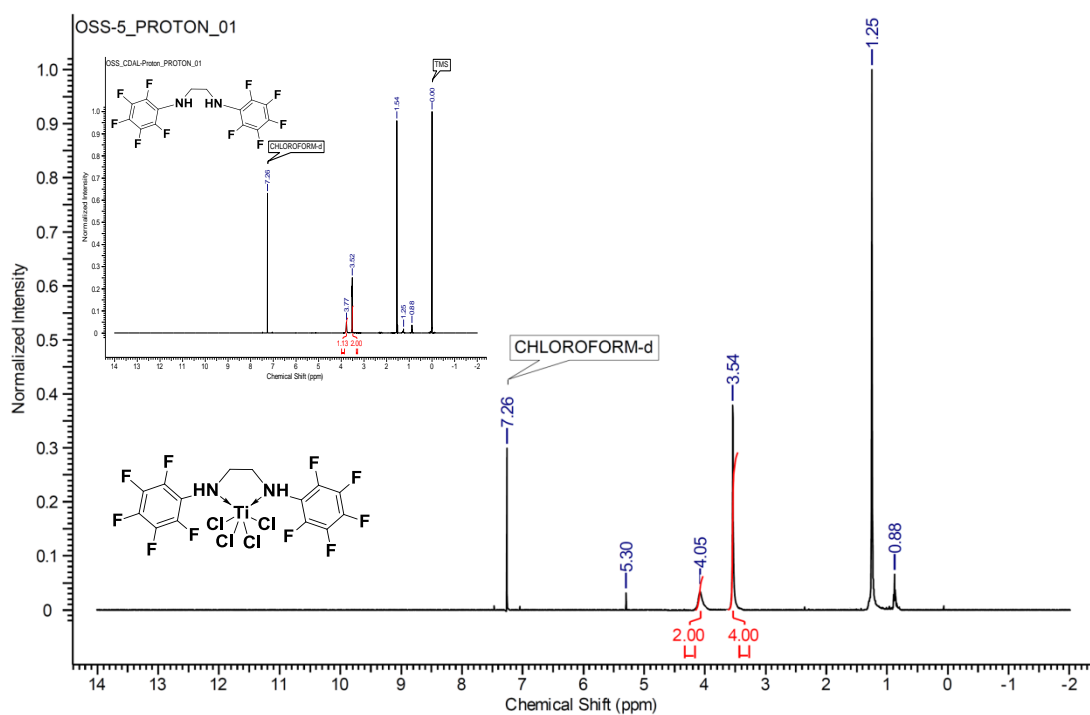
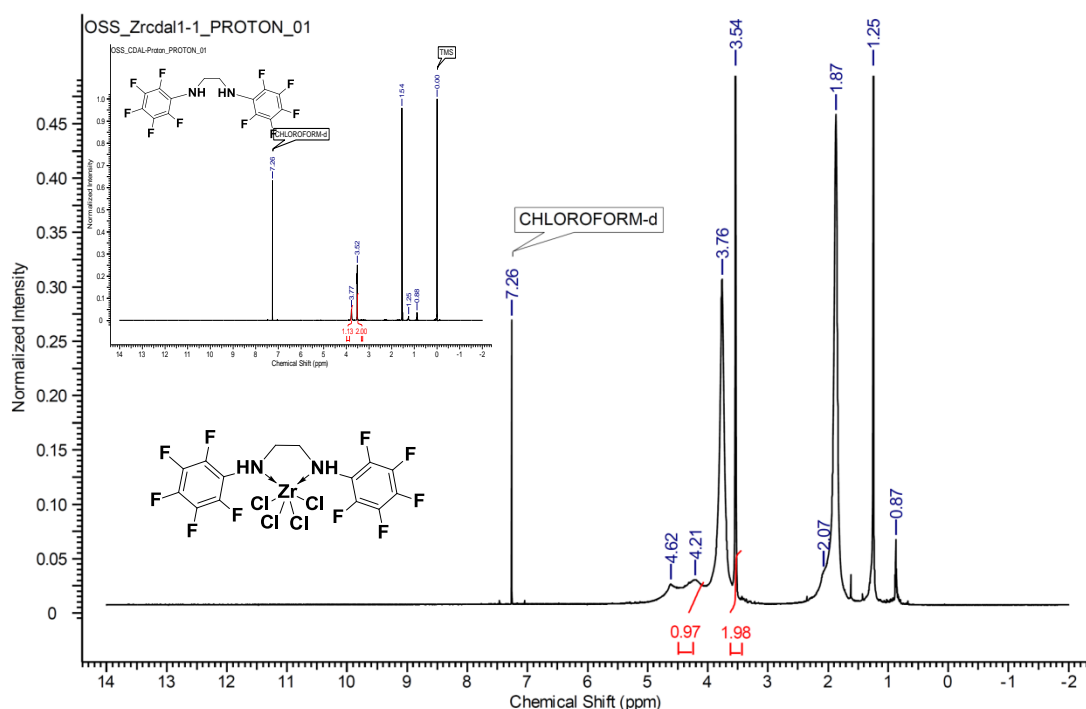


Figure 4.4: <sup>1</sup>H-NMR spectra of **1** and **2**.

#### 4.2.1.2 Tetrachloro N,N-bis(perfluorophenyl)ethane-1,2-diamine Zirconium (IV), (**3**):

According to FT-IR datum of **3**, *NH* stretching band, Ar*FNH*-CH<sub>2</sub>-CH<sub>2</sub>-*NH*Ar*F*, was shifted to 3232 cm<sup>-1</sup> due to coordination via lone-pair electrons of nitrogen atoms to

zirconium. electrons on nitrogen atoms. The FT-IR spectrum of **3** was shown in **Fig. A.23**. According to  $^1\text{H-NMR}$  spectrum of **3**,  $\text{CH}_2$  protons,  $\text{ArFNH-CH}_2\text{-CH}_2\text{-NHArF}$ , shifted 0.02 ppm to downfield and were observed at 3.54 ppm.  $\text{NH}$  protons,  $\text{ArFNH-CH}_2\text{-CH}_2\text{-NHArF}$ , shifted 0.45 ppm to downfield and were observed at 4.21 ppm which was reasonable due to the coordination of nitrogen atoms to zirconium. The  $^1\text{H-NMR}$  spectrum of **3** was shown in **Fig. 4.5** and **Fig. A.6**. According to  $^{19}\text{F-NMR}$  spectrum of **3**,  $\text{ArF}$  signals,  $\text{ArFNH-CH}_2\text{-CH}_2\text{-NHArF}$ , shifted around 1 ppm to downfield. The  $^{19}\text{F-NMR}$  spectrum of **3** was shown in **Fig. A.16**.



**Figure 4.5:**  $^1\text{H-NMR}$  spectra of **1** and **3**.

#### 4.2.1.3 Tetrachloro N,N-bis(perfluorophenyl)ethane-1,2-diamine Hafnium (IV), (**4**):

According to  $^1\text{H-NMR}$  spectrum of **4**,  $\text{CH}_2$  protons,  $\text{ArFNH-CH}_2\text{-CH}_2\text{-NHArF}$ , shifted 0.07 ppm to downfield and were observed at 3.59 ppm.  $\text{NH}$  protons,  $\text{ArFNH-CH}_2\text{-CH}_2\text{-NHArF}$ , shifted over 1 ppm to downfield and were observed at 4.81 ppm which was reasonable due to the coordination of nitrogen atoms to hafnium. The  $^1\text{H-NMR}$  spectrum of **4** was shown in **Fig. 4.6** and **Fig. A.7**. According to  $^{19}\text{F-NMR}$  spectrum of **4**,  $\text{ArF}$  signals,  $\text{ArFNH-CH}_2\text{-CH}_2\text{-NHArF}$ , shifted greater to downfield in comparison to **2** and **3**. The  $^{19}\text{F-NMR}$  spectrum of **4** was shown in **Fig. A.17**.

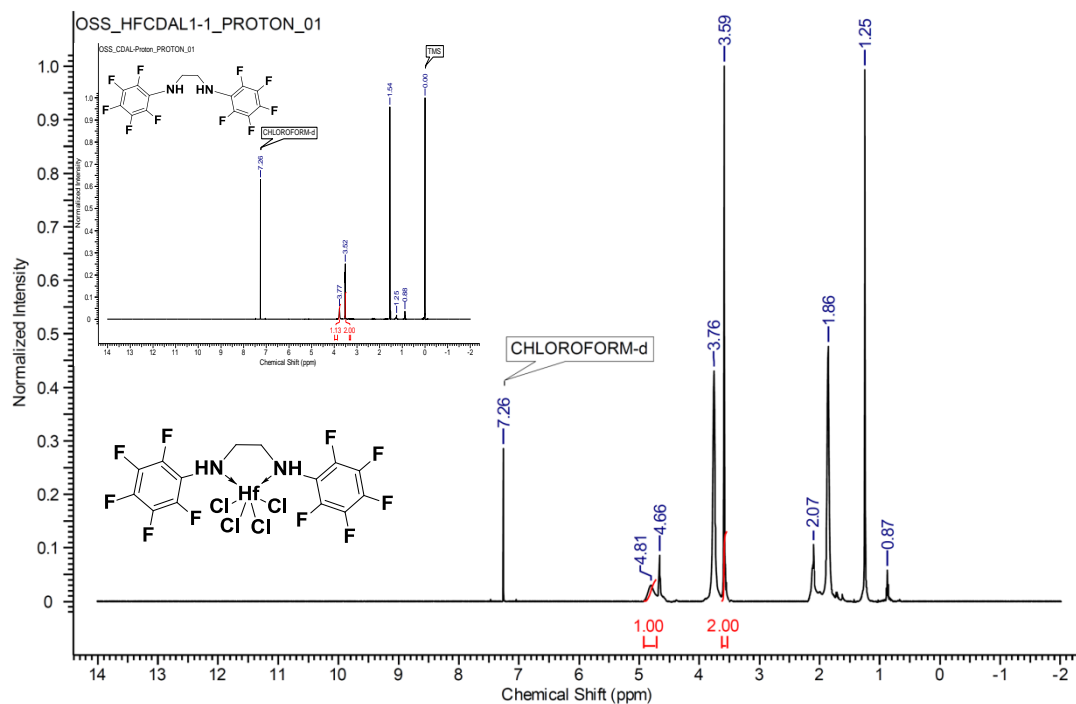


**Figure 4.6:**  $^1\text{H-NMR}$  spectra of **1** and **4**.

#### 4.2.2 Via a Reaction Between $\text{MCl}_4$ ( $\text{M} = \text{Ti}, \text{Zr}, \text{Hf}$ ) and Disodium 1,2-diylbis((perfluorophenyl)amide)ethane

Disodium salt of N,N-bis(perfluorophenyl)ethane-1,2-diamine was prepared by the reaction between **1** and  $\text{NaH}$  and characterized by  $^1\text{H-NMR}$  methods.  $\text{MCl}_2\text{L}^-\text{L}$  type of complexes were prepared by the reaction between  $\text{MCl}_4$  ( $\text{M}: \text{Ti}, \text{Zr}, \text{Hf}$ ) and disodium of  $\text{L}^-\text{L}$  salt, ( $\text{L}^-\text{L}$ : 1,2-diylbis((perfluorophenyl)amide)ethane) in THF. The complexes were characterized by using FT-IR,  $^1\text{H-NMR}$  and  $^{19}\text{F-NMR}$  methods.

##### 4.2.2.1 Disodium 1,2-diylbis((perfluorophenyl)amide)ethane, (**5**):

According to  $^1\text{H-NMR}$  spectrum of **5**,  $\text{NH}$  protons,  $\text{ArFN-CH}_2\text{-CH}_2\text{-NArF}$ , disappeared in comparison to N,N-bis(perfluorophenyl)ethane-1,2-diamine. Due to NH bond cleavage, the bonding electrons remained on nitrogen atoms and gained negative charge. Nitrogen atoms of amide were attracted by sodium cations and attracted CN bonding electrons that is why the  $\text{CH}_2$  protons,  $\text{ArFN-CH}_2\text{-CH}_2\text{-NArF}$ , shifted 0.2 ppm to downfield and were observed at 3.72 ppm. The  $^1\text{H-NMR}$  spectrum of **5** was shown in **Fig. 4.7** and **Fig. A.8**.

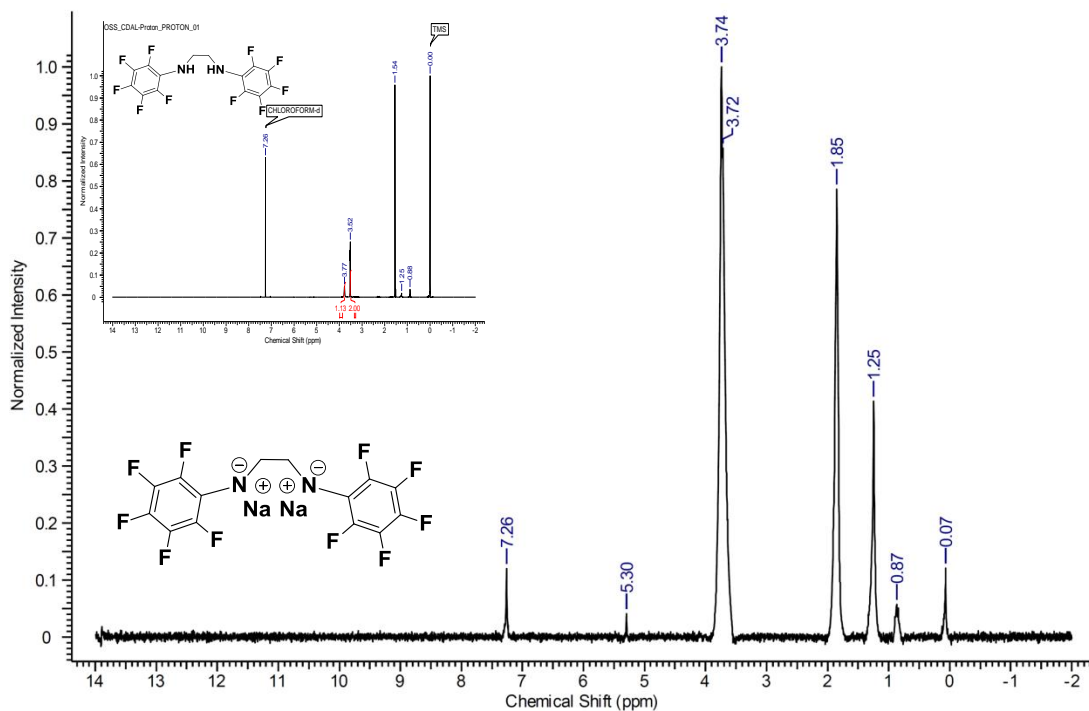


Figure 4.7:  $^1\text{H}$ -NMR spectra of **1** and **5**.

#### 4.2.2.2 Dichloro 1,2-diylbis((perfluorophenyl)amide)ethane Zirconium (IV), (**6**):

According to FT-IR datum of **1**,  $\text{CN}$ ,  $\text{FAr-NH-CH}_2\text{-CH}_2\text{-HN-ArF}$ , aromatic stretching band of  $\text{N,N-bis(perfluoro phenyl) ethane-1,2-diamine}$  was observed at  $1326\text{ cm}^{-1}$ . By the formation of **6**,  $\text{CN}$ ,  $\text{FAr-N-CH}_2\text{-CH}_2\text{-N-ArF}$ , aromatic stretching band shifted to  $1365\text{ cm}^{-1}$ . The FT-IR spectrum of **6** was shown in **Fig. 4.8** and **Fig. A.24**. According to  $^1\text{H}$ -NMR spectrum of **6**,  $\text{CH}_2$  protons,  $\text{ArFN-CH}_2\text{-CH}_2\text{-NArF}$ , shifted  $0.63\text{ ppm}$  to downfield and were observed at  $4.35\text{ ppm}$ . A new sigma bond formed between nitrogen atoms and zirconium due to  $\text{NH}$  bond cleavage. The  $^1\text{H}$ -NMR spectrum of **6** was shown in **Fig. 4.9** and **Fig. A.9**. According to  $^{19}\text{F}$ -NMR of **6**, due to sigma bonding between nitrogen atoms and zirconium, greater shifts in  $\text{ArF}$ ,  $\text{ArFN-CH}_2\text{-CH}_2\text{-NArF}$ , were observed in comparison to the complexes **2**, **3**, **4**. The reason of these shifts could also be caused by the interaction between  $o$ -fluorine atoms and zirconium. The  $^{19}\text{F}$ -NMR spectrum of **6** was shown in **Fig. A.18**.

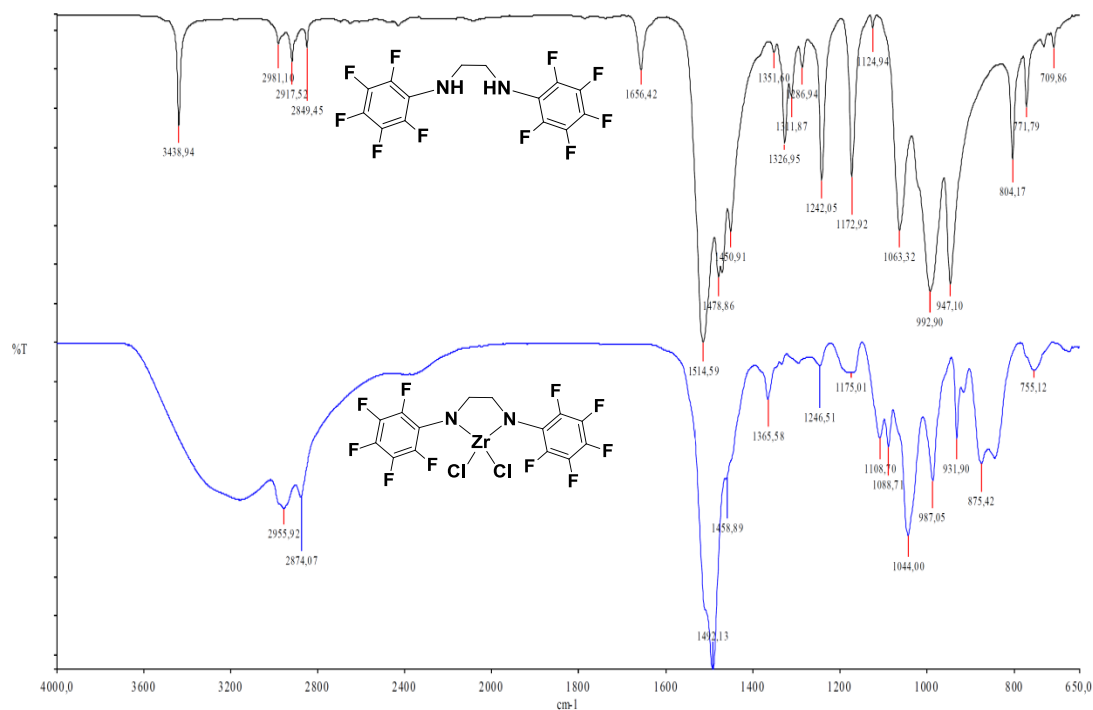


Figure 4.8: FT-IR spectra of **1** and **6**.

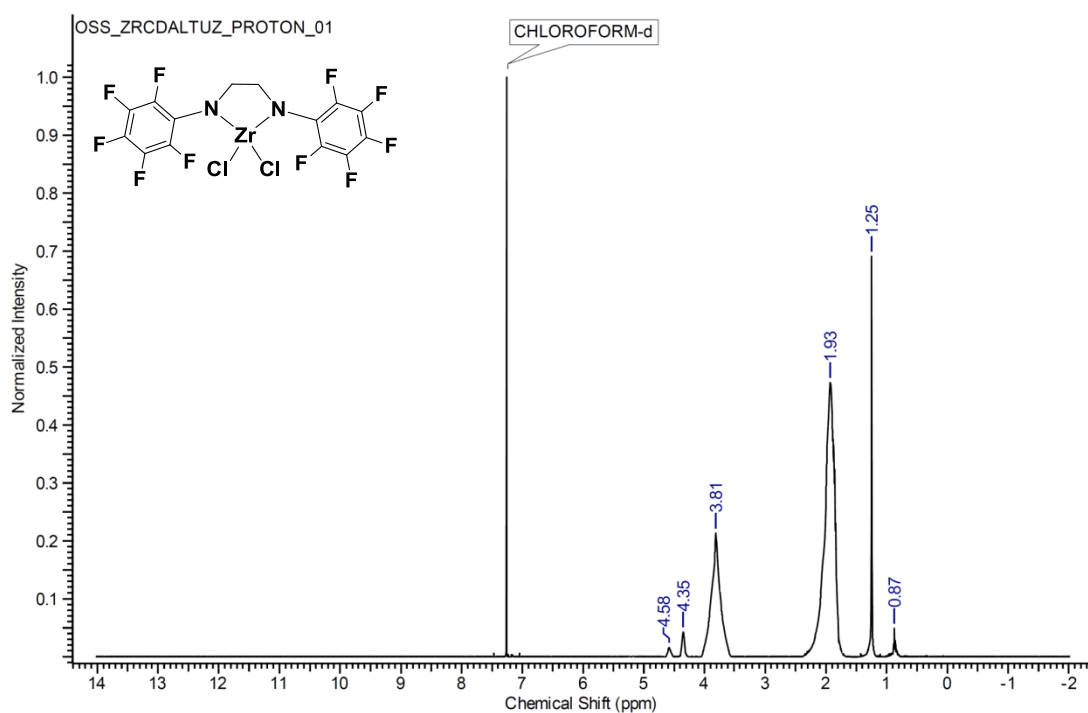
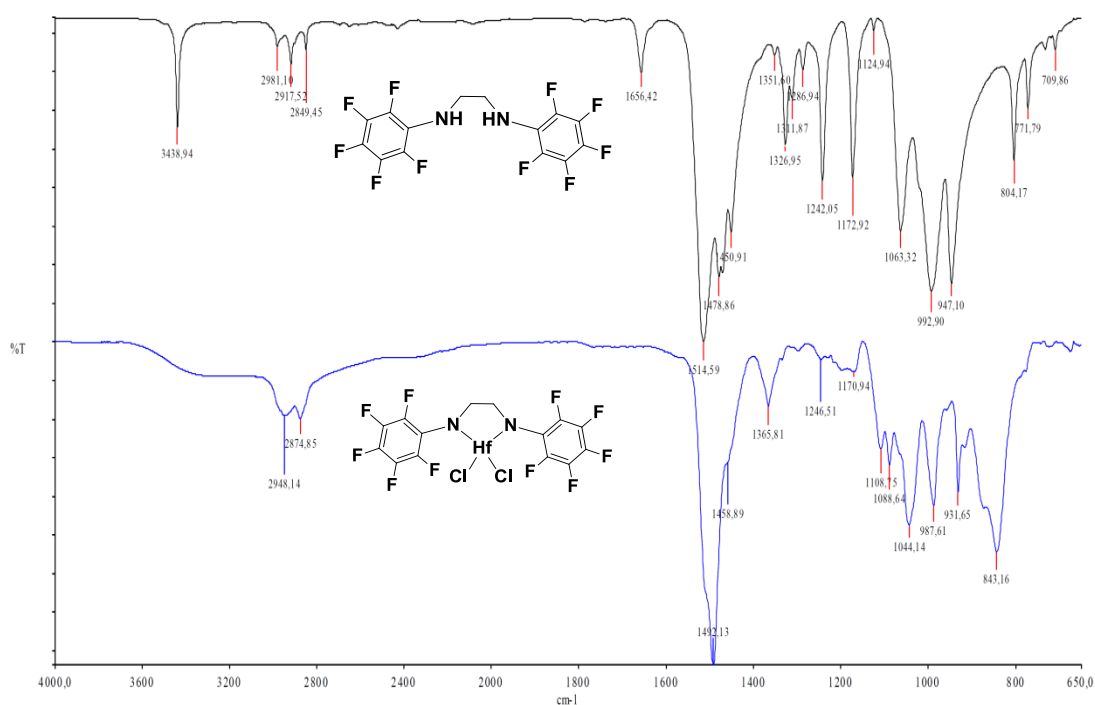


Figure 4.9:  $^1\text{H-NMR}$  spectrum of **6**.

#### 4.2.2.3 Dichloro 1,2-diylbis((perfluorophenyl)amide)ethane Hafnium (IV), (**7**):

According to FT-IR datum of **1**, *CN*, *F**Ar*-NH-CH<sub>2</sub>-CH<sub>2</sub>-HN-*Ar**F*, aromatic stretching band of *N,N*-bis(perfluoro phenyl) ethane-1,2-diamine was observed at

1326  $\text{cm}^{-1}$ . By the formation of **6**, *CN*, *F*Ar-N-CH<sub>2</sub>-CH<sub>2</sub>-N-ArF, aromatic stretching band shifted to 1365  $\text{cm}^{-1}$ . The FT-IR spectrum of **7** was shown in **Fig. 4.10** and **Fig. A.25**. According to <sup>1</sup>H-NMR spectrum of **7**, CH<sub>2</sub> protons, ArFN-CH<sub>2</sub>-CH<sub>2</sub>-NArF, shifted 0.67 ppm to downfield and were observed at 4.39 ppm. A new sigma bond formed between nitrogen atoms and hafnium due to NH bond cleavage. The <sup>1</sup>H-NMR spectrum of **7** was shown in **Fig. 4.11** and **Fig. A.10**. According to <sup>19</sup>F-NMR of **6**, due to sigma bonding between nitrogen atoms and hafnium, greater shifts in *ArF*, *ArFN*-CH<sub>2</sub>-CH<sub>2</sub>-N*ArF*, were observed in comparison to the complexes **2**, **3**, **4**. The reason of these shifts could also be caused by the interaction between *o*-fluorine atoms and zirconium. The <sup>19</sup>F-NMR spectrum of **6** was shown in **Fig. A.19**.



**Figure 4.10:** FT-IR spectra of **1** and **7**.

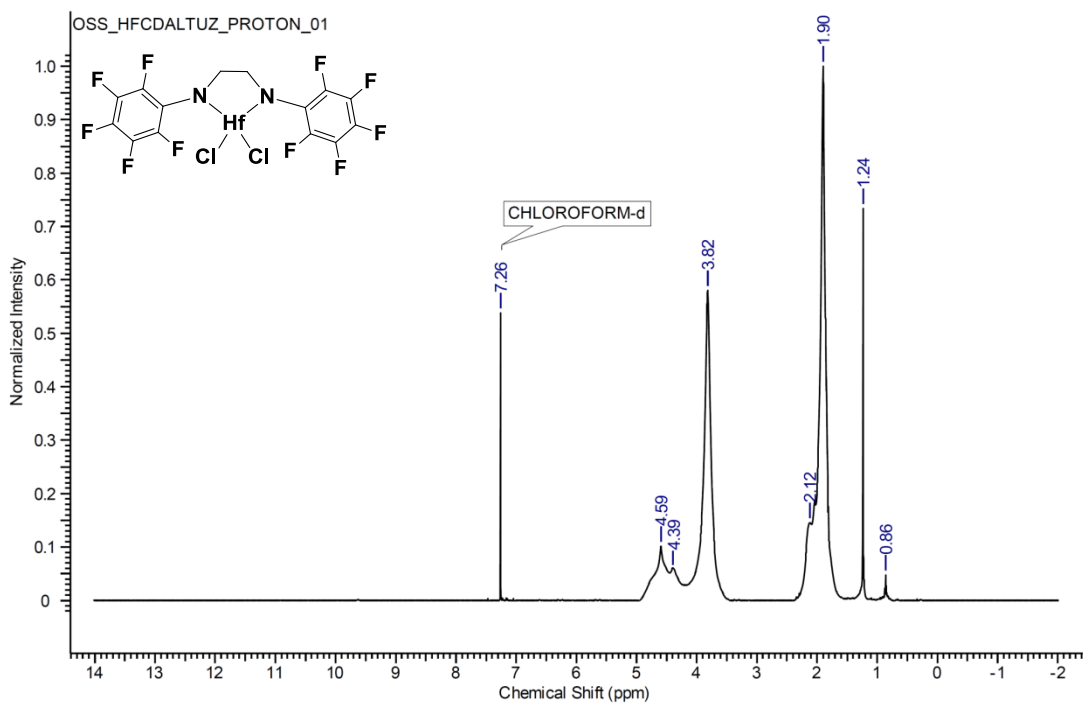


**Figure 4.11:**  $^1\text{H}$ -NMR spectrum of **7**.

## 5. CONCLUSION

A novel highly fluorinated nitrogen-based chelating diamine ligand was synthesized and characterized by various spectroscopic methods.  $MCl_4L^L$  type of complexes of this new diamine ligand were prepared by the direct reaction between  $MCl_4$  (M: Ti, Zr, Hf) and N,N-bis(perfluorophenyl)ethane-1,2-diamine in  $CH_2Cl_2$  or THF. These complexes were characterized by FT-IR,  $^1H$ -NMR and  $^{19}F$ -NMR methods. Spectroscopic evidences proved that a coordination occurred to metal (M: Ti, Zr, Hf) atom via non-bonding electrons on nitrogen atoms.  $MCl_2L^L$  type of complexes of this new diamine ligand were prepared by the reaction of  $MCl_4$  (M: Zr, Hf) with the disodium salt of new diamine ligand  $Na_2(ArFN-CH_2-CH_2-NArF)$  which was produced by the reaction between diamine ligand and excess sodium hydride (NaH). All the spectroscopic evidences proved that the chelation of diamine ligand to metal (M: Zr, Hf atom) occurred via sigma bondings of the nitrogen atoms. The electron withdrawing groups in ligand are expected to increase the electrophilicity of the metal centre. Increased electrophilic character of the metal centre enhances the tendency to interact with olefins [18, 19]. THF coordination to central metal (M: Ti, Zr, Hf) atoms is very common and can be removed from the complexes by refluxing either in benzene or toluene. We assume that complexes **6** and **7** are possible and efficient precatalyst candidates for olefin polymerization.



## REFERENCES

- [1] **Severn, J. R. ; Chadwick, J. C.**, 2008: Tailor-made polymers: via immobilization of alpha-olefin polymerization; *Wiley-VCH: Weinheim*
- [2] **Guan, Z.**, 2009: Metal Catalysts in Olefin Polymerization; *Springer-Verlag: Berlin Heidelberg*
- [3] **Gupta, K. C.; Sutar, A. K.**, 2008: Catalytic activities of Schiff base transition metal complexes, *Coordination Chemistry Reviews*, **252**, 1420.
- [4] **Agapie, T.; Henling, L. M.; DiPasquale, A. G.; Rheingold, A. L.; Bercaw, J. E.**, 2008: Zirconium and Titanium Complexes Supported by Tridentate LX2 Ligands Having Two Phenolates Linked to Furan, Thiophene, and Pyridine Donors: Precatalysts for Propylene Polymerization and Oligomerization; *Organometallics*, **27**, 6245.
- [5] **Kissin, Y. V.**, 2008: Alkene Polymerization Reactions with Transition Metal Catalysts; *Elsevier*
- [6] **Chirik, P. J.**, 2010: Group 4 Transition Metal Sandwich Complexes: Still Fresh after Almost 60 Years, *Organometallics*, **29**, 1500.
- [7] **Talsi, E. P.; Bryliakov, K. P.; Semikolenova, N. V.; Zakharov, V. A.; Bochmann, M.**, 2007: Key intermediates in metallocene-and post-metallocene-catalyzed polymerization, *Kinetics and Catalysis*, **48**, 490.
- [8] **Gurubasavaraj, P. M.; Roesky, H. W.; Nekoueishahraki, B.; Pal, A.; Herbst-Irmer, R.**, 2008: From unstable to stable: Half-metallocene catalysts for olefin polymerization, *Inorganic Chemistry*, **47**, 5324.
- [9] **Gibson, V. C.; Spitzmesser, S. K.**, 2003: Advances in non-metallocene olefin polymerization catalysis, *Chemical Reviews*, **103**, 283.
- [10] **Kuran, W.**, 2001: Principles of Coordination Polymerization; *Wiley-VCH: Weinheim*.
- [11] **Rappe, A. T.; Skiff, W. M.; Casewit, C. J.**, 2000: Modeling metal-catalyzed olefin polymerization, *Chemical Reviews*, **100**, 1435.
- [12] **Tynys, A.; Saarinen, T.; Hakala, K.; Helaja, T.; Vanne, T.; Lehmus, P.; Lofgren, B.**, 2005: Ethylene-propylene copolymerisations: Effect of metallocene structure on termination reactions and polymer microstructure, *Macromolecular Chemistry and Physics*, **206**, 1043.

- [13] **Tam, K. H.; Chan, M. C. W.; Kaneyoshi, H.; Makio, H.; Zhu, N. Y.**, 2009: Indirect Substituent Effects upon the Olefin Polymerization Reactivity of Titanium(IV) Chelating  $\sigma$ -Aryl Catalysts *Organometallics*, **28**, 5877.
- [14] **Matsui, S.; Fujita, T.**, 2001: FI Catalysts: super active new ethylene polymerization catalysts, *Catalysis Today*, **66**, 63.
- [15] **Song, D. P.; Wu, J. Q.; Ye, W. P.; Mu, H. L.; Li, Y. S.**, 2010: Accessible, Highly Active Single-Component beta-Ketiminato Neutral Nickel(II) Catalysts for Ethylene Polymerization, *Organometallics*, **29**, 2306.
- [16] **Bryliakov, K. P.; Talsi, E. P.; Moller, H. M.; Baier, M. C.; Mecking, S.**, 2010: Noncovalent Interactions in o-Fluorinated Post-titanocene Living Ethylene Polymerization Catalyst, *Organometallics*, **29**, 4428.
- [17] **Marquet, N.; Kirillov, E.; Roisnel, T.; Razavi, A.; Carpentier, J. F.**, 2009: Group 4 Metal Complexes of Fluorous (Di)Alkoxide - (Di)Imino Ligands: Synthesis, Structure, Olefin Polymerization Catalysis, and Decomposition Pathways, *Organometallics*, **28**, 606.
- [18] **Lee, W. Y.; Liang, L. C.**, 2008: Fluorinated diarylamido complexes of lithium, zirconium, and hafnium, *Inorganic Chemistry*, **47**, 3298.
- [19] **Campora, J.; Matas, I.; Palma, P.; Alvarez, E.; Kleijn, H.; Deelman, B. J.; Passaglia, E.**, 2010: Highly fluorous zirconocene (IV) complexes and their catalytic applications in the polymerization of ethylene, *Journal of Organometallic Chemistry*, **695**, 1794.
- [20] **Ziniuk, Z.; Goldberg, I.; Kol, M.**, 1999: Zirconium Complexes of Chelating Dianionic bis (pentafluorophenylamido) ligands: synthesis, structure and ethylene polymerisation activity, *Inorganic Chemistry Comm.*, **2**, 549-551.
- [21] **Scollard, J. D.; McConville, D. H.; Vittal, J. J.; Payne, N. C.**, 1998: Chelating Diamide Complexes of Titanium: New Catalyst Precursors for the Highly Active and Living Polymerization of  $\alpha$ -Olefins, *Journal of molecular Catalysis A: Chemical*, **128**, 201-214.
- [22] **Turculet, L.; Tilley, T. D.**, 2002: Zirconium amide, halide, and alkyl complexes supported by tripodal amido ligands derived from cis,cis-1,3,5-triaminocyclohexane, *Organometallics*, **21**, 3961.
- [23] **O'Connor, P. E.; Morrison, D. J.; Steeves, S.; Burrage, K.; Berg, D. J.**, 2001: Zirconium complexes of fluorinated aryl diamides, *Organometallics*, **20**, 1153.
- [24] **Tsurugi, H.; Matsuo, Y.; Yamagata, T.; Mashima, K.**, 2004: Intramolecular benzylation of an imino group of tridentate 2,5-bis(N-aryliminomethyl)pyrrolyl ligands bound to zirconium and hafnium gives amido-pyrrolyl complexes that catalyze ethylene polymerization, *Organometallics*, **23**, 2797.

[25] **Holland, D.G.; Moore, G.J.; Tamborski, C.**, 1964: Preparation and Reactions of Mydrazino Perfluoroaromatic Compounds, *Journal of Organic Chemistry*, **29**, 1562.



## APPENDICES

### APPENDIX A.1 GC-MS Data:

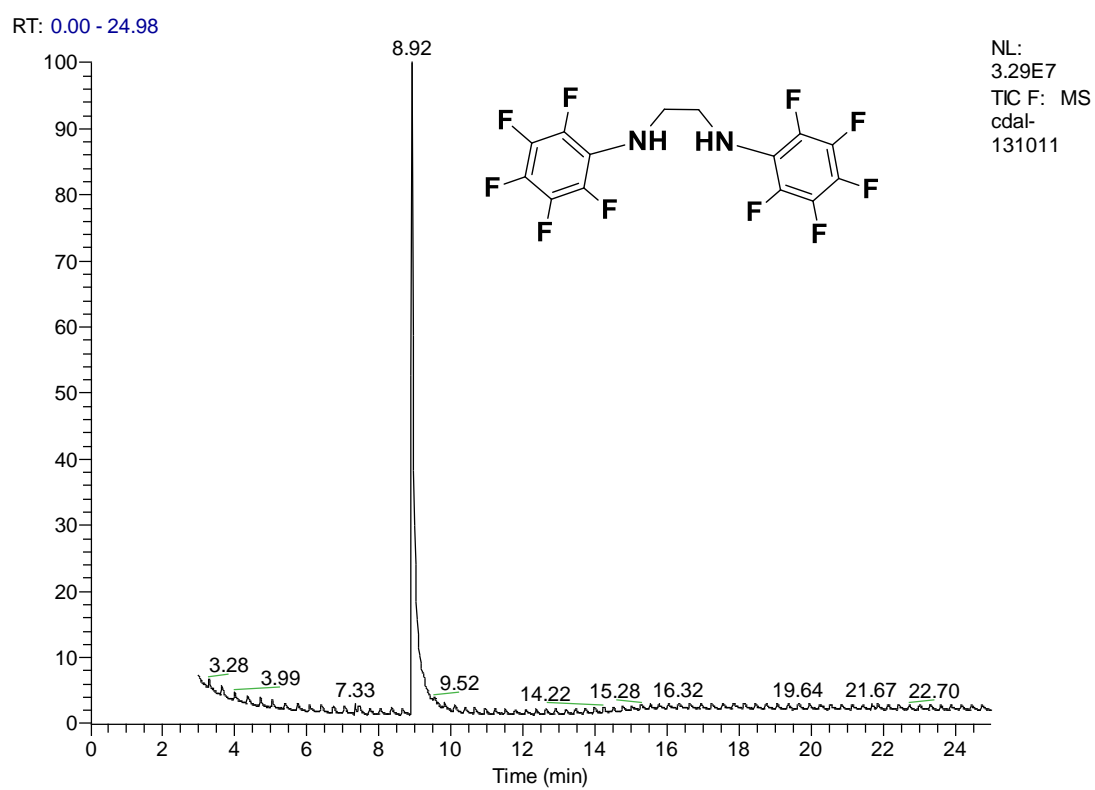


Figure A.1 : Gas Chromatogram of **1**.

cdal-131011 #258 RT: 8.92 AV: 1 NL: 1.55E7  
T: + c Full ms [ 20.00-700.00]

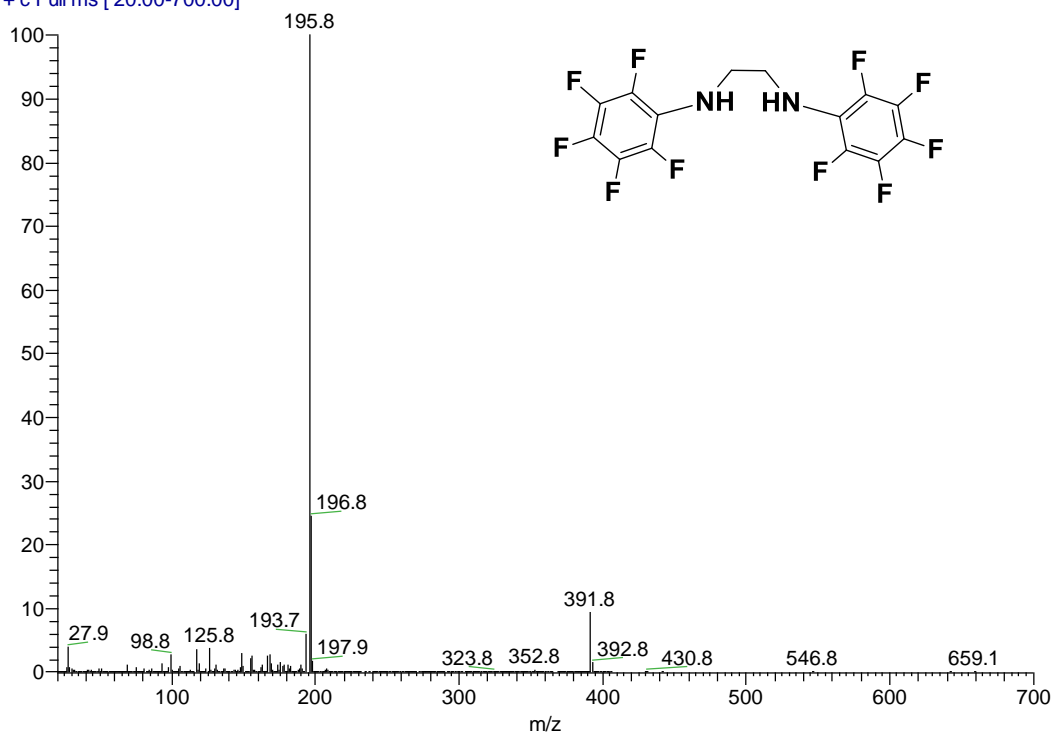


Figure A.2 : Mass Spectrum of 1.

### APPENDIX A.2 <sup>1</sup>H-NMR Spectra:

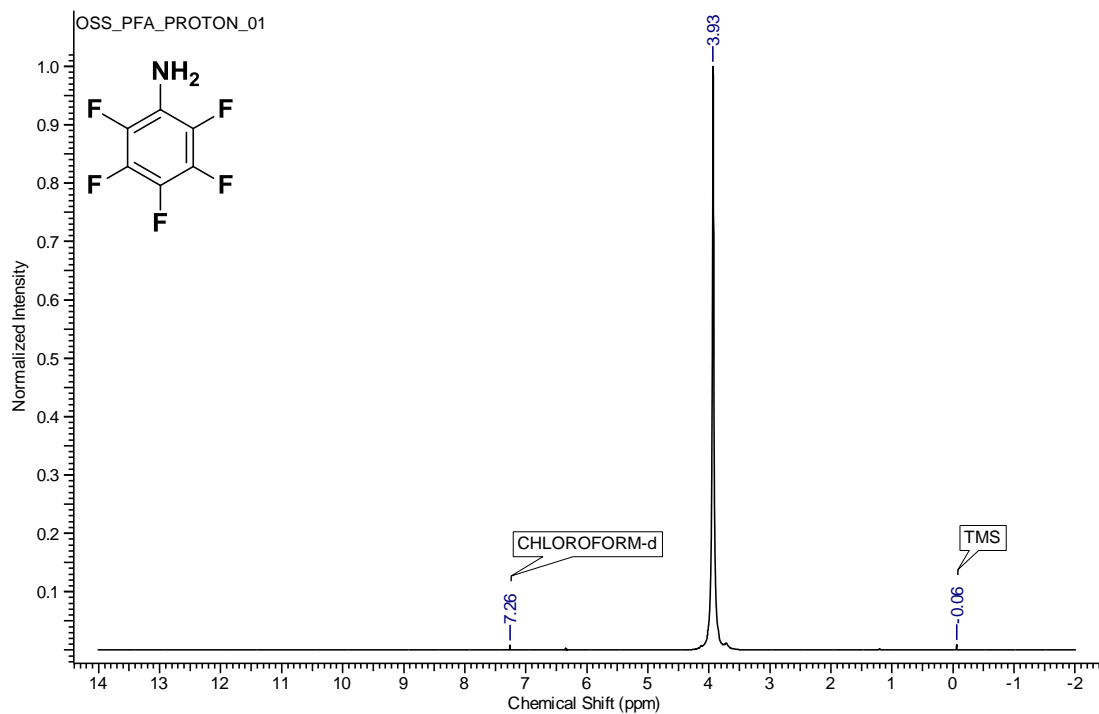


Figure A.3 : <sup>1</sup>H-NMR spectrum of PFA.

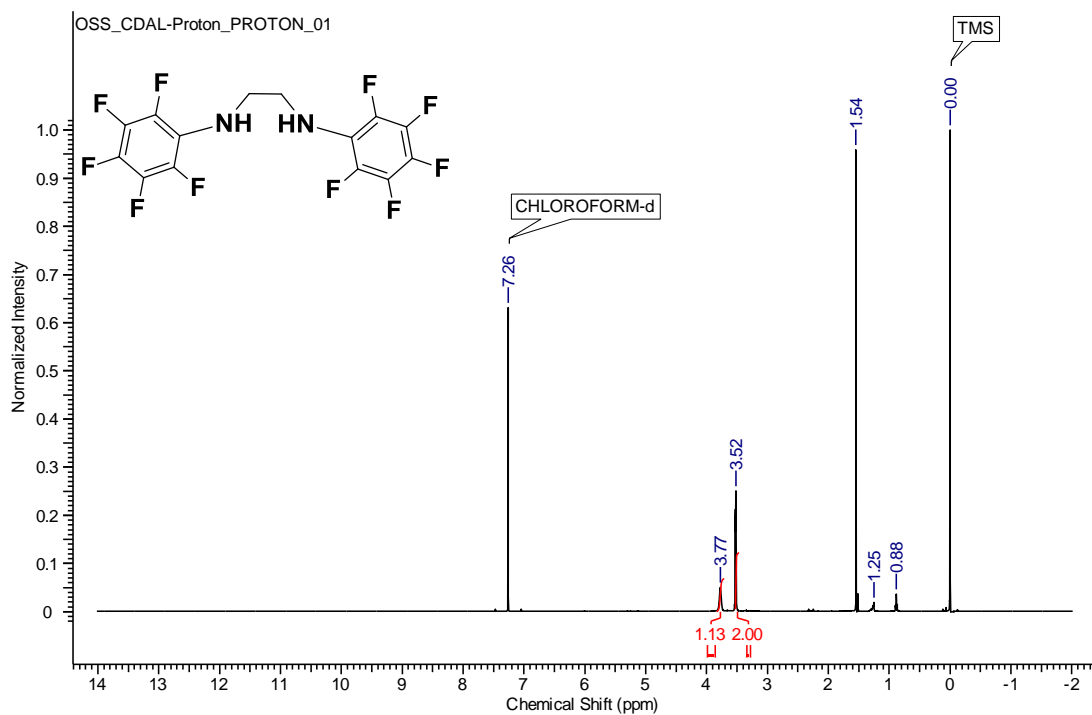


Figure A.4 :  $^1\text{H}$ -NMR spectrum of **1**.

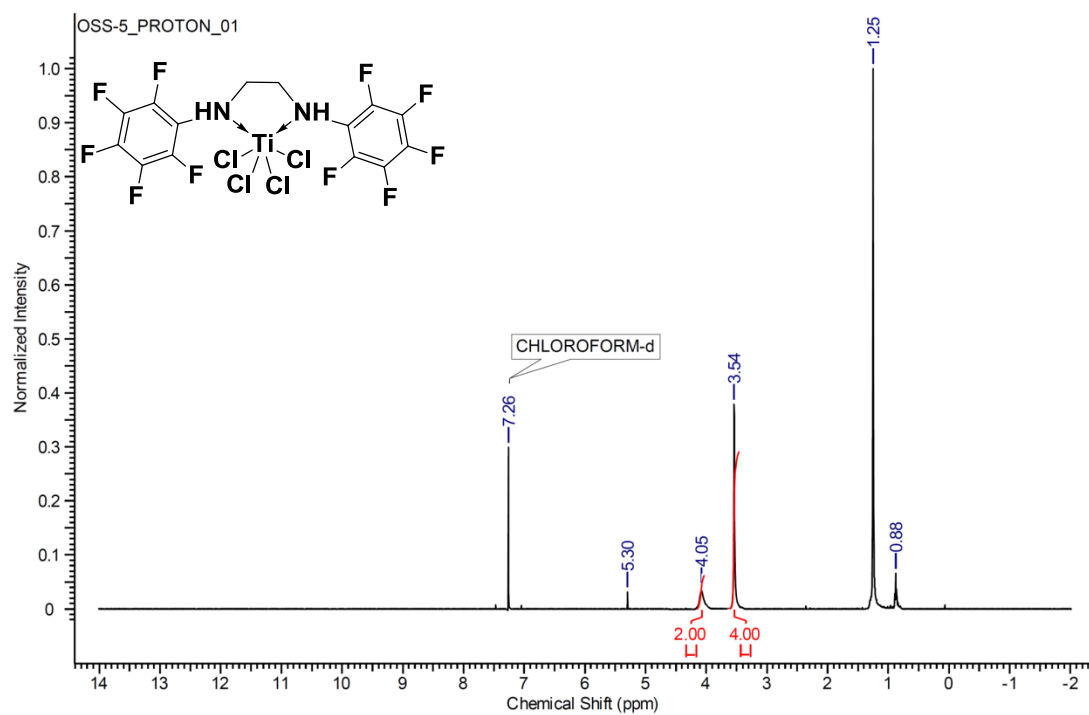


Figure A.5 :  $^1\text{H}$ -NMR spectrum of **2**.

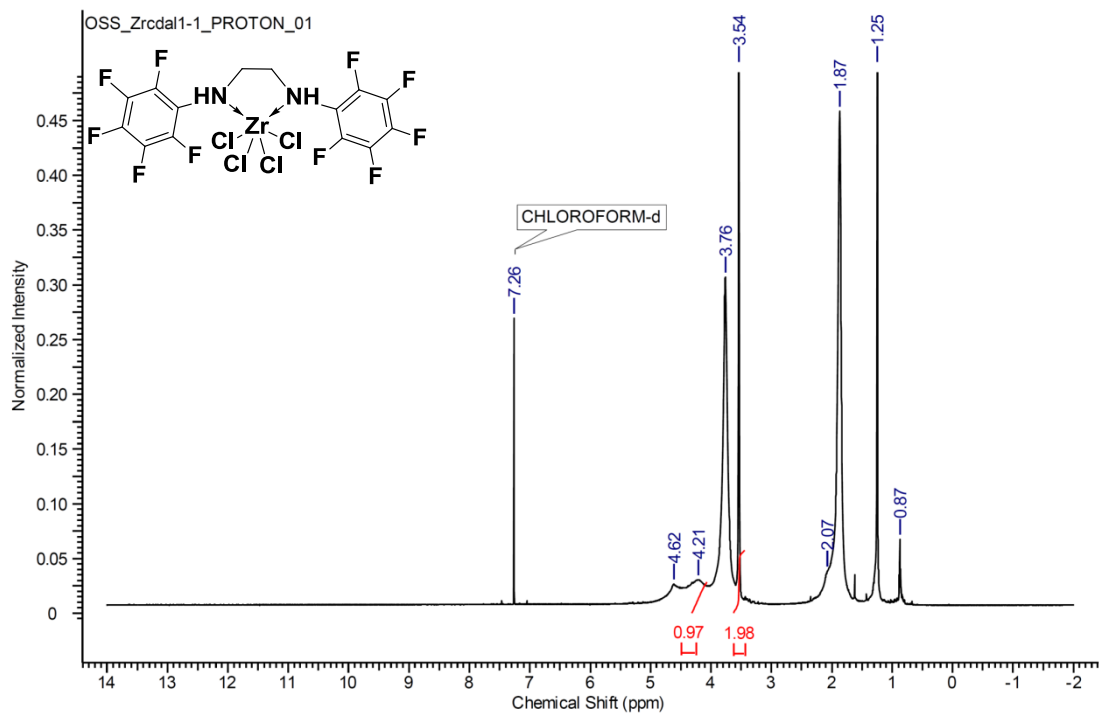


Figure A.6 :  $^1\text{H}$ -NMR spectrum of **3**.

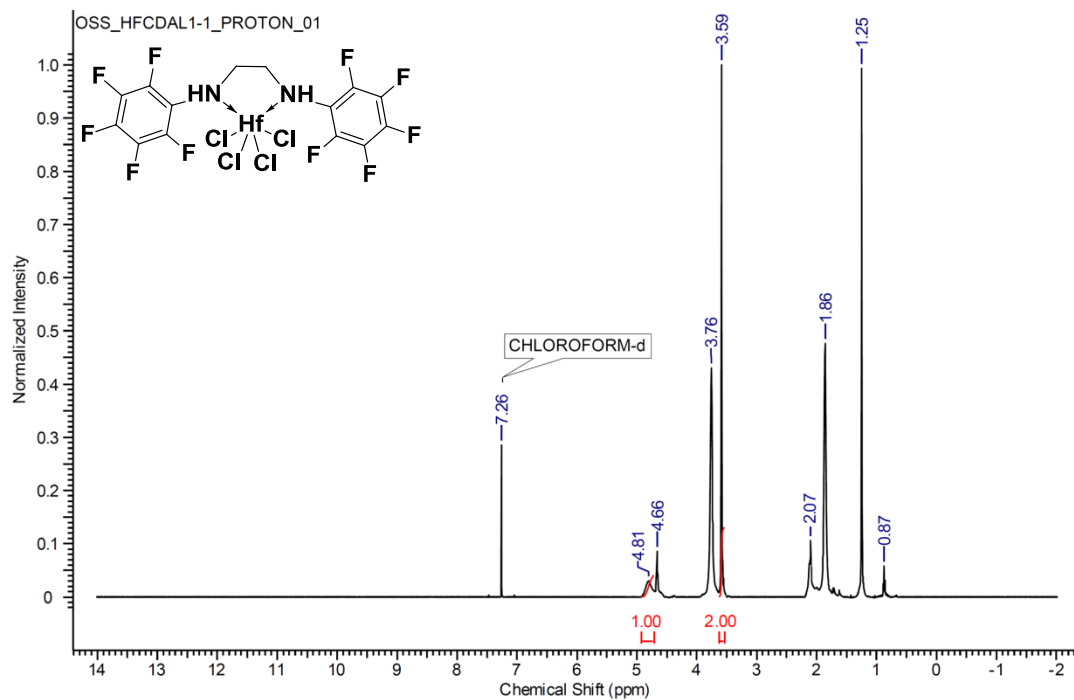


Figure A.7 :  $^1\text{H}$ -NMR spectrum of **4**.

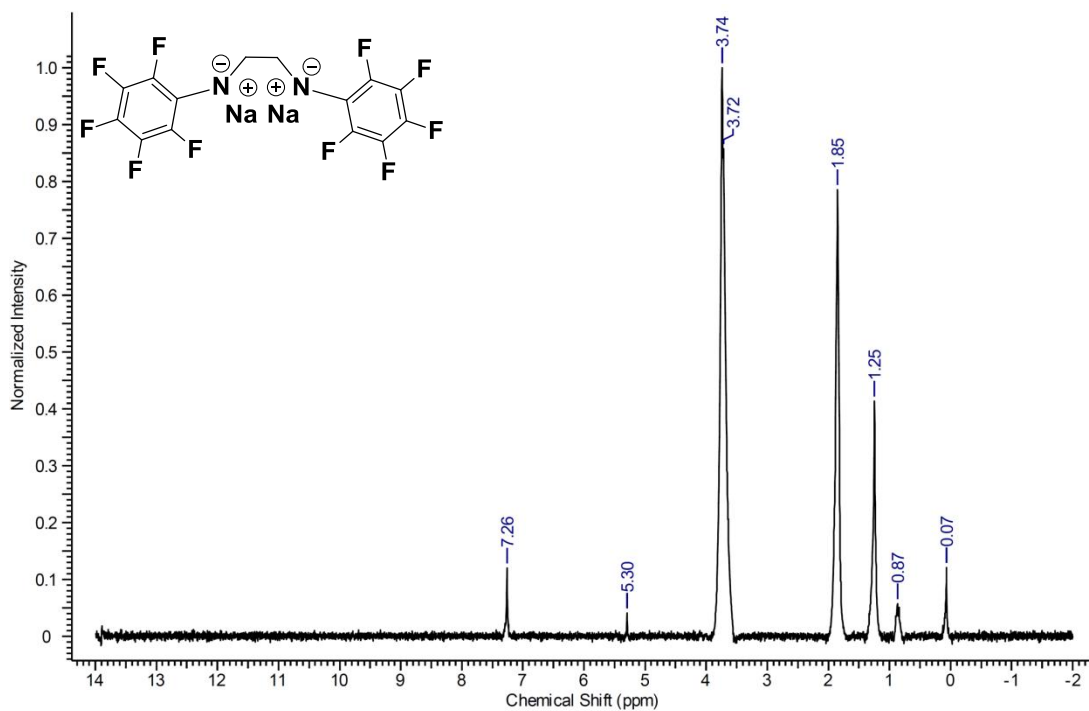


Figure A.8 :  $^1\text{H-NMR}$  spectrum of **5**.

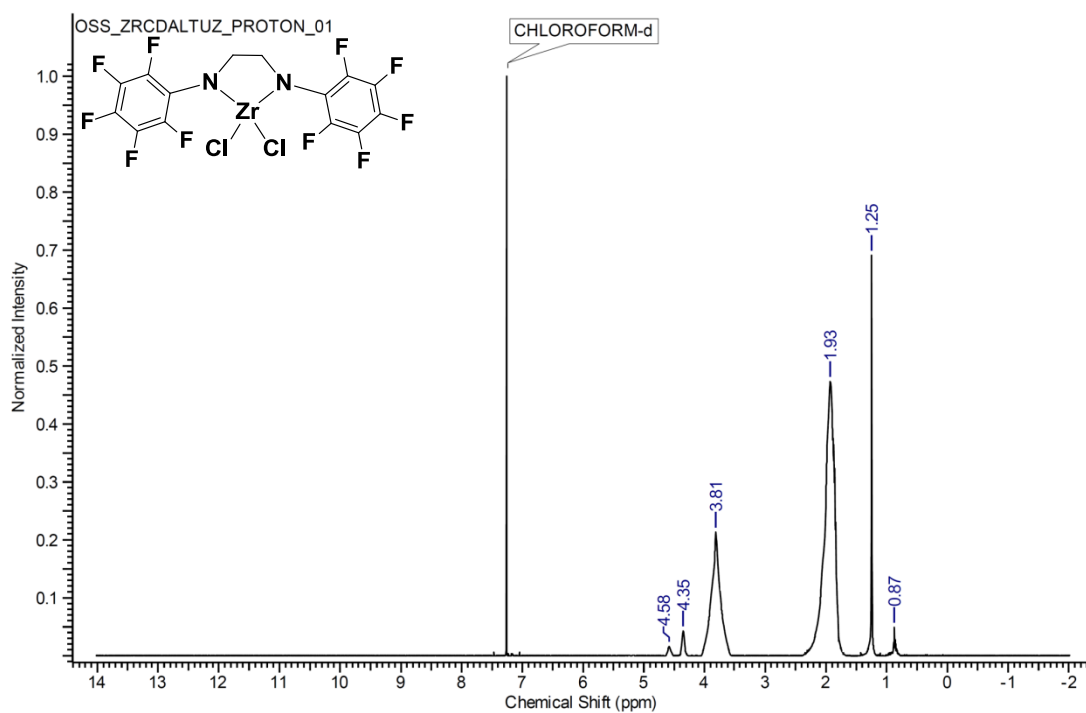


Figure A.9 :  $^1\text{H-NMR}$  spectrum of **6**.

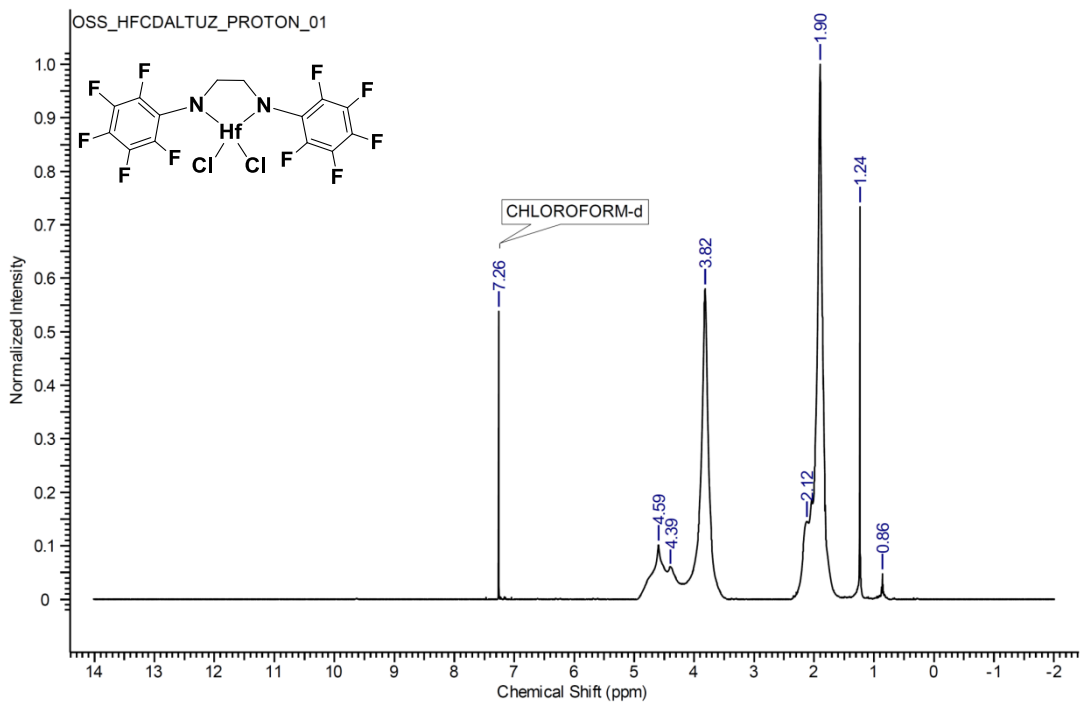


Figure A.10 :  $^1\text{H}$ -NMR spectrum of **7**.

APPENDIX A.3  $^{13}\text{C}$ -NMR Spectra:

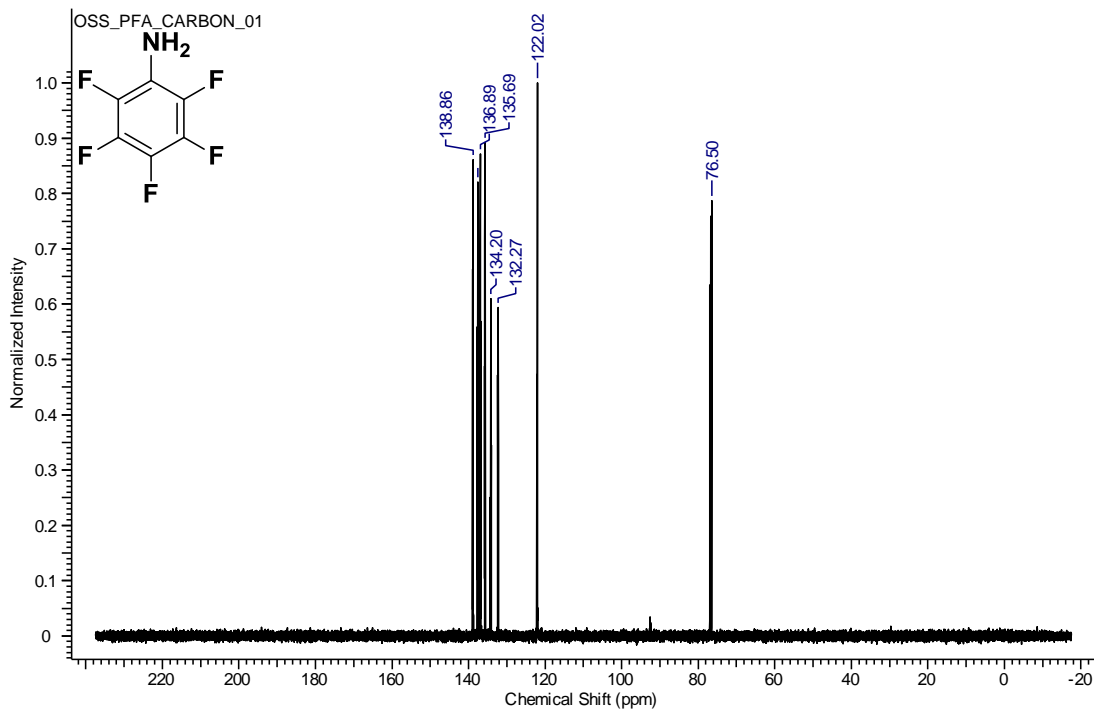


Figure A.11 :  $^{13}\text{C}$ -NMR spectrum of **PFA**.

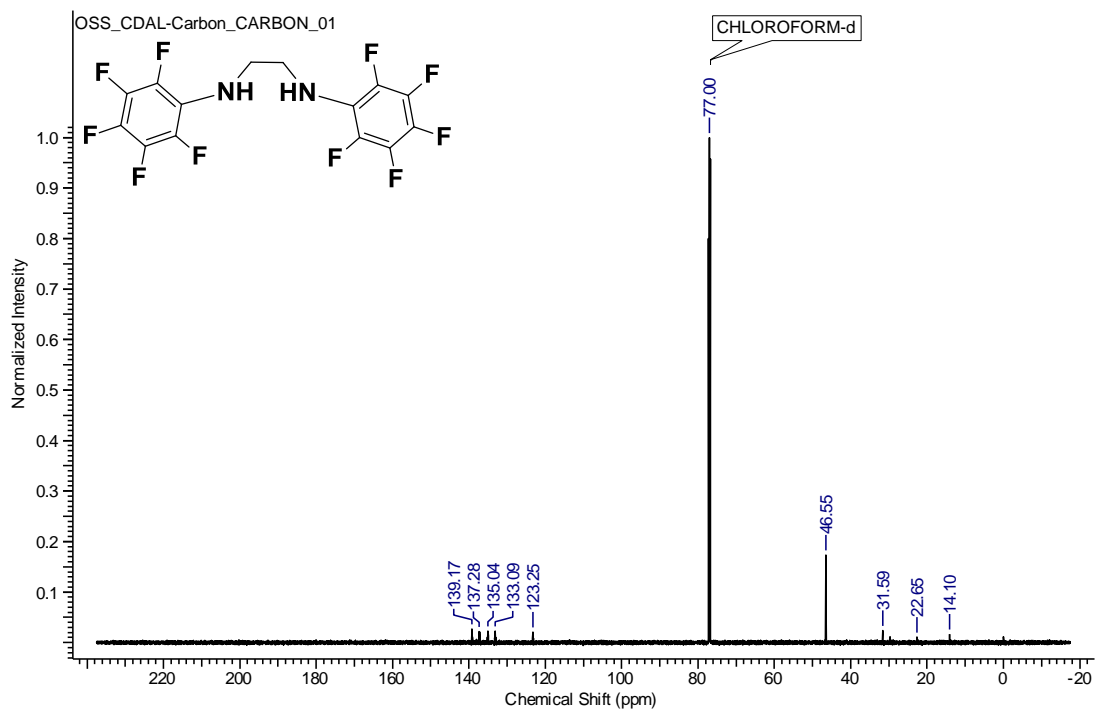


Figure A.12 :  $^{13}\text{C}$ -NMR spectrum of **1**.

#### APPENDIX A.4 $^{19}\text{F}$ -NMR Spectra:

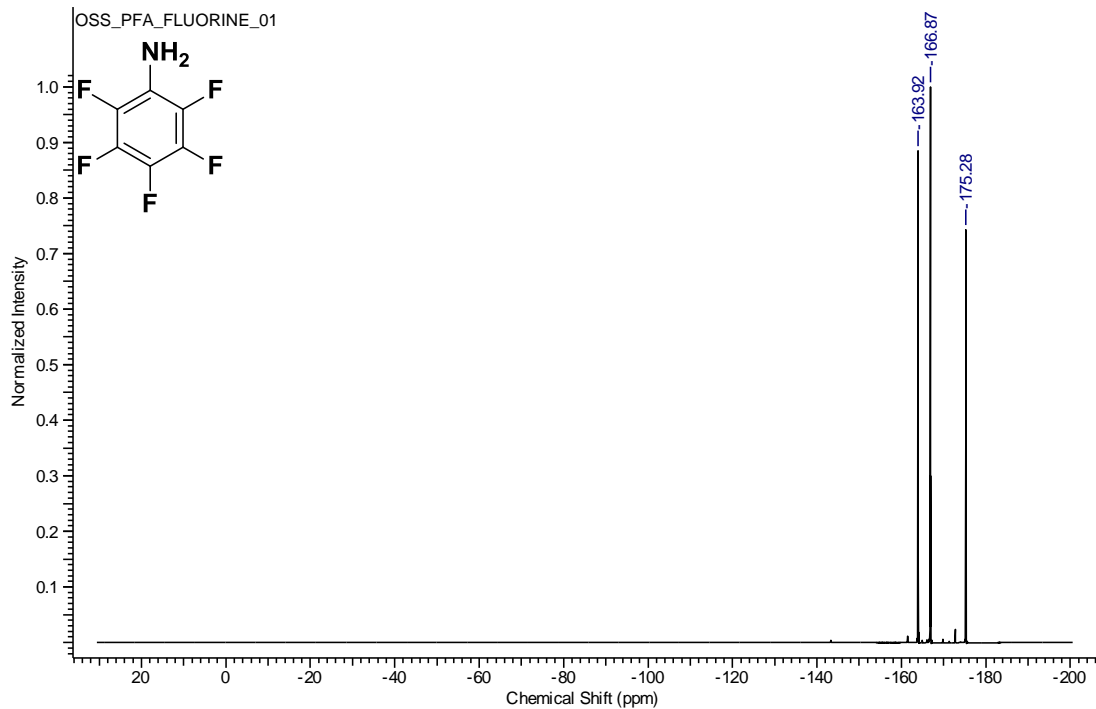


Figure A.13 :  $^{19}\text{F}$ -NMR spectrum of PFA.

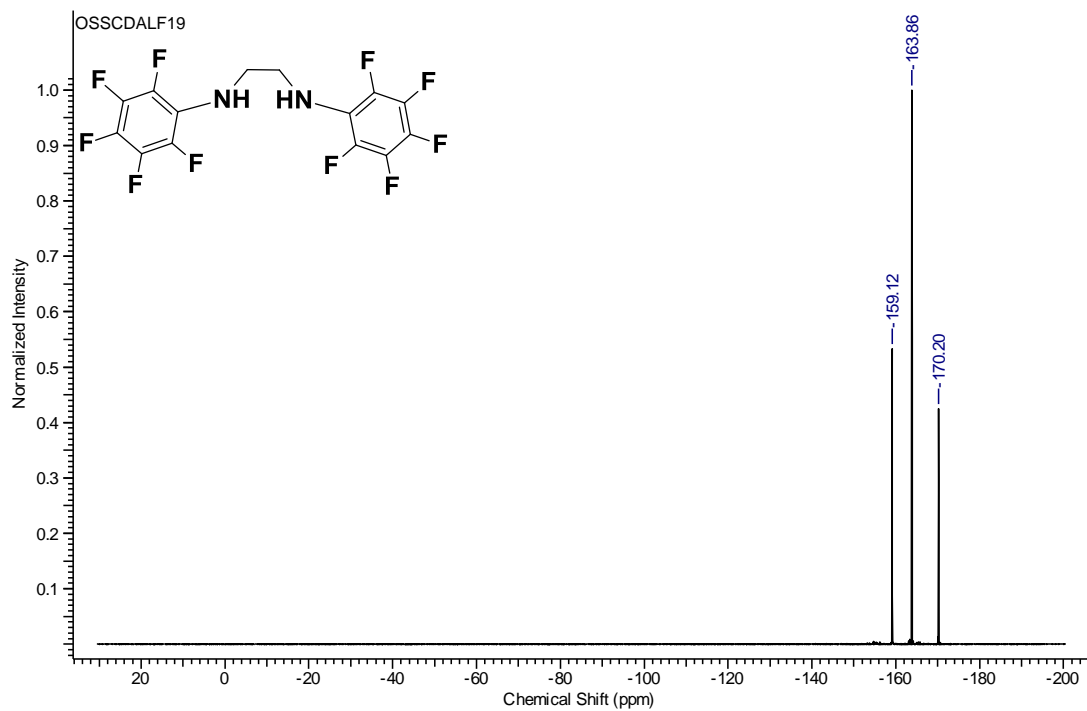


Figure A.14 :  $^{19}\text{F}$ -NMR spectrum of **1**.

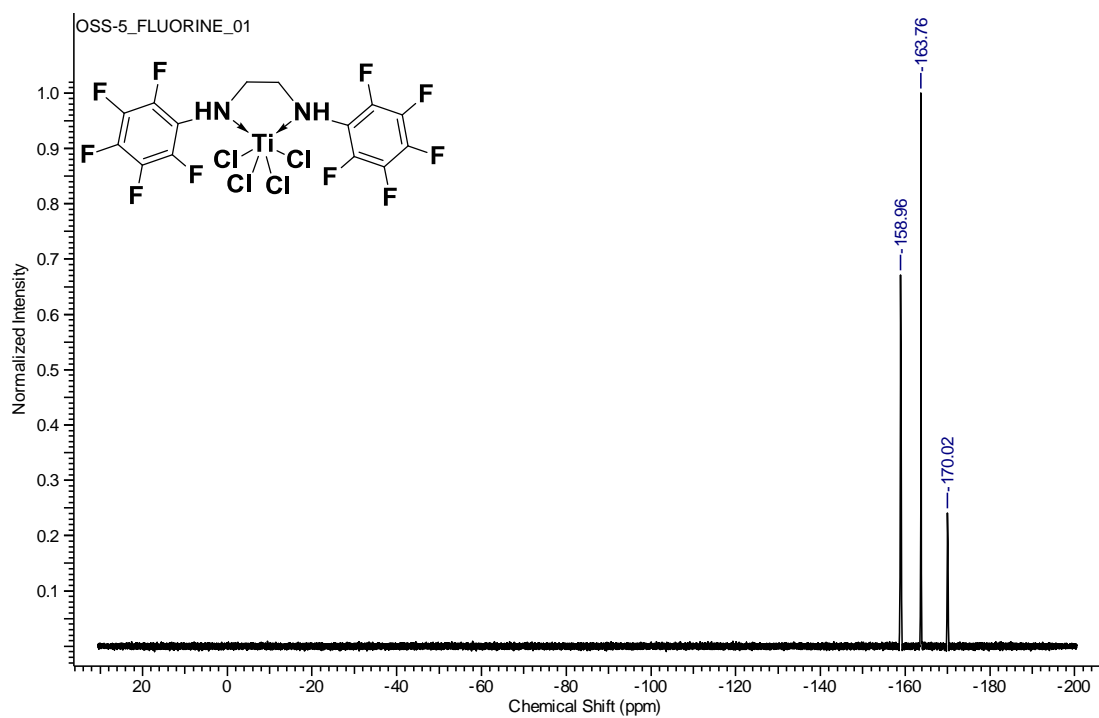


Figure A.15 :  $^{19}\text{F}$ -NMR spectrum of **2**.

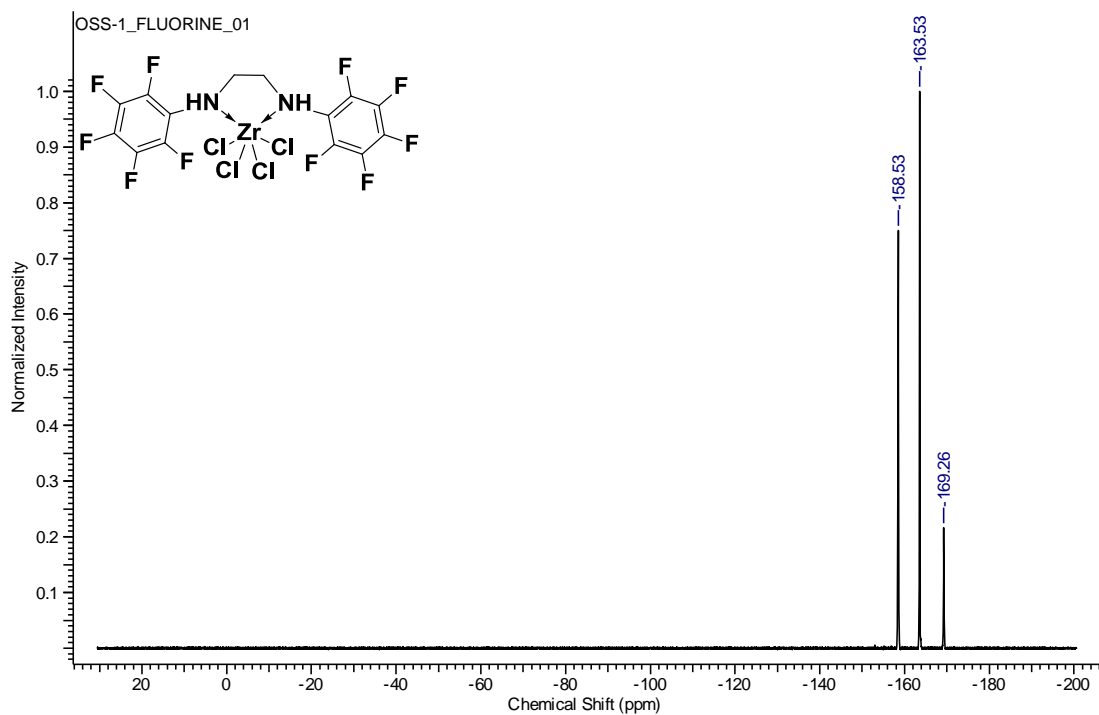


Figure A.16 :  $^{19}\text{F}$ -NMR spectrum of **3**.

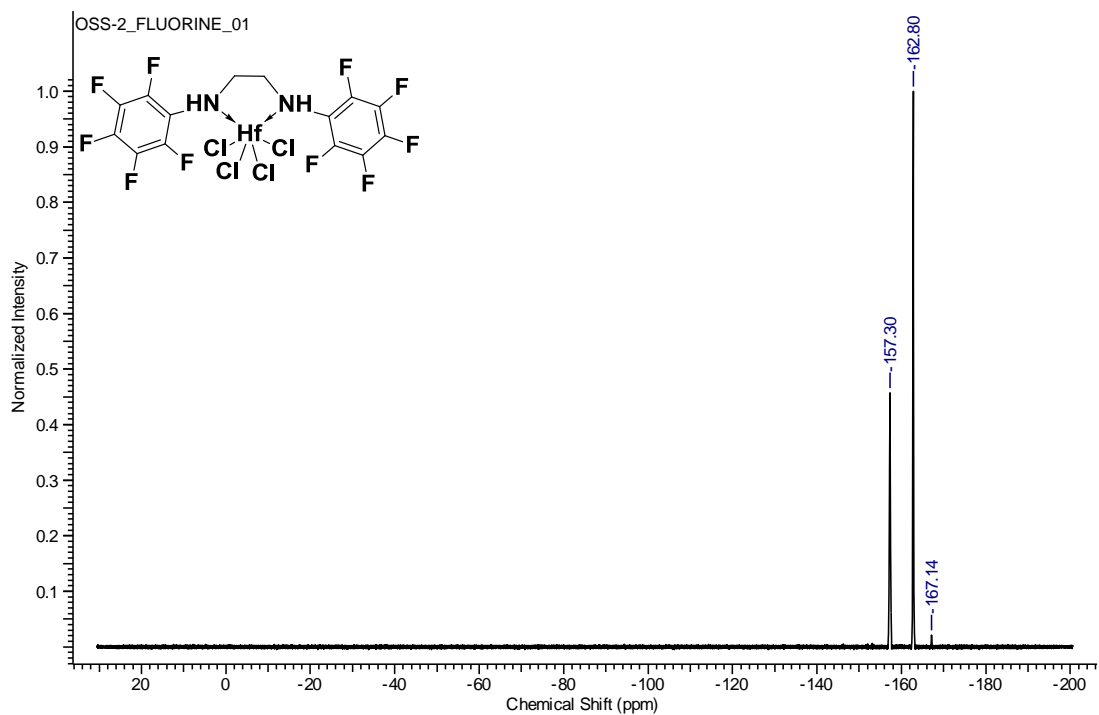


Figure A.17 :  $^{19}\text{F}$ -NMR spectrum of **4**.

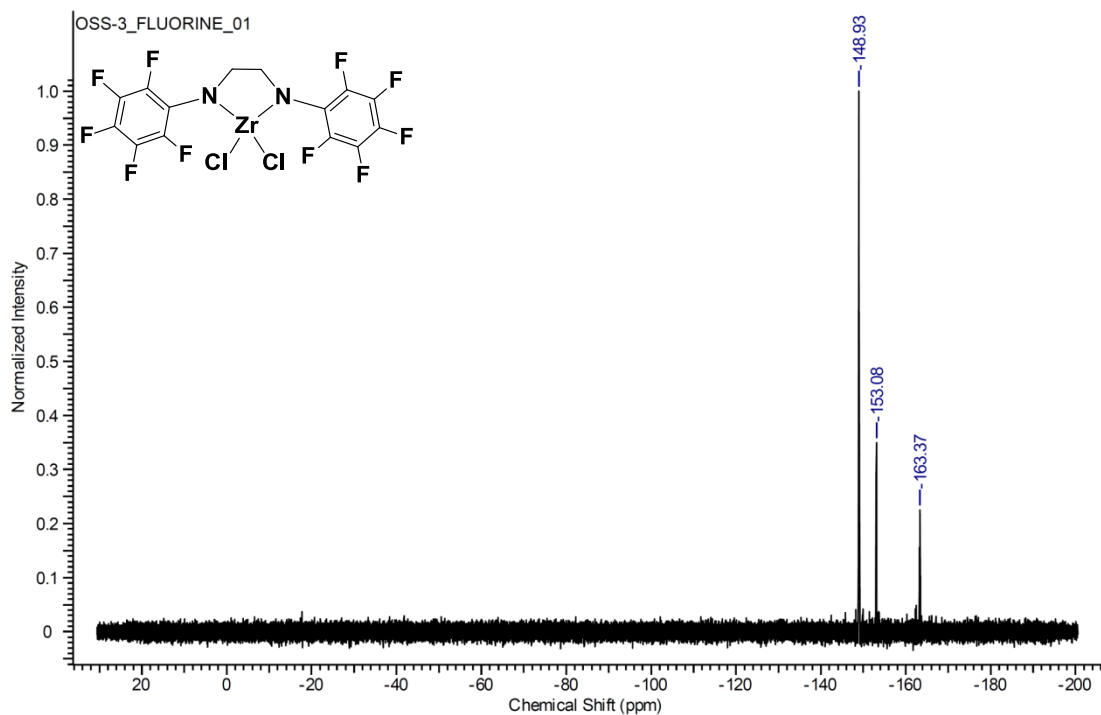


Figure A.18 :  $^{19}\text{F}$ -NMR spectrum of **6**.

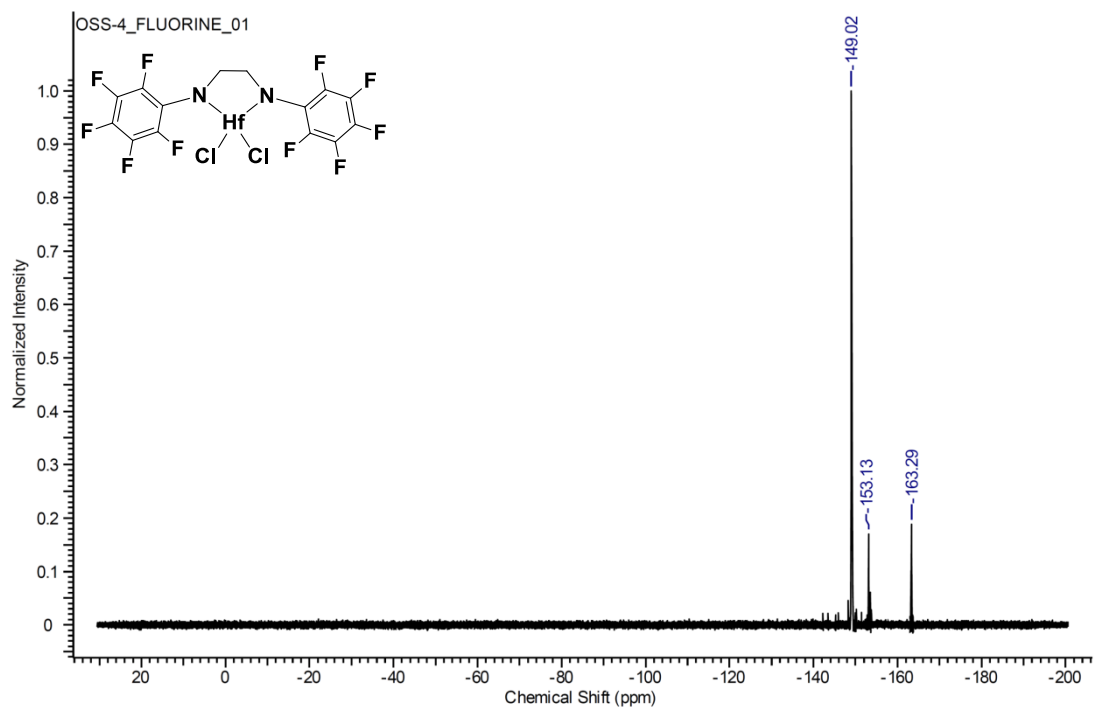


Figure A.19 :  $^{19}\text{F}$ -NMR spectrum of **7**.

## APPENDIX A.5 FT-IR Spectra:

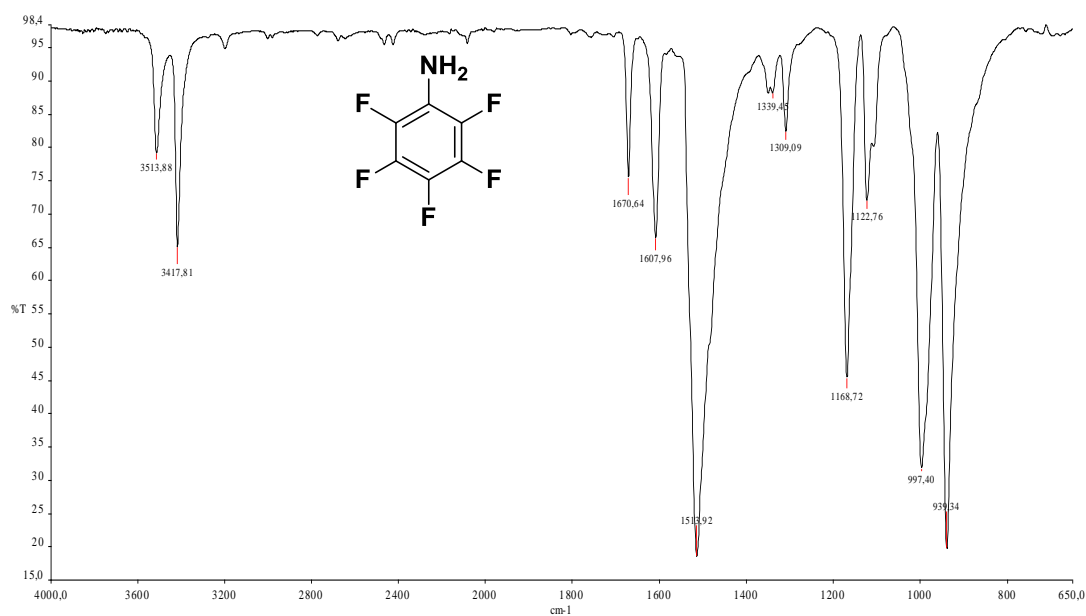


Figure A.20 : FT-IR spectrum of PFA.

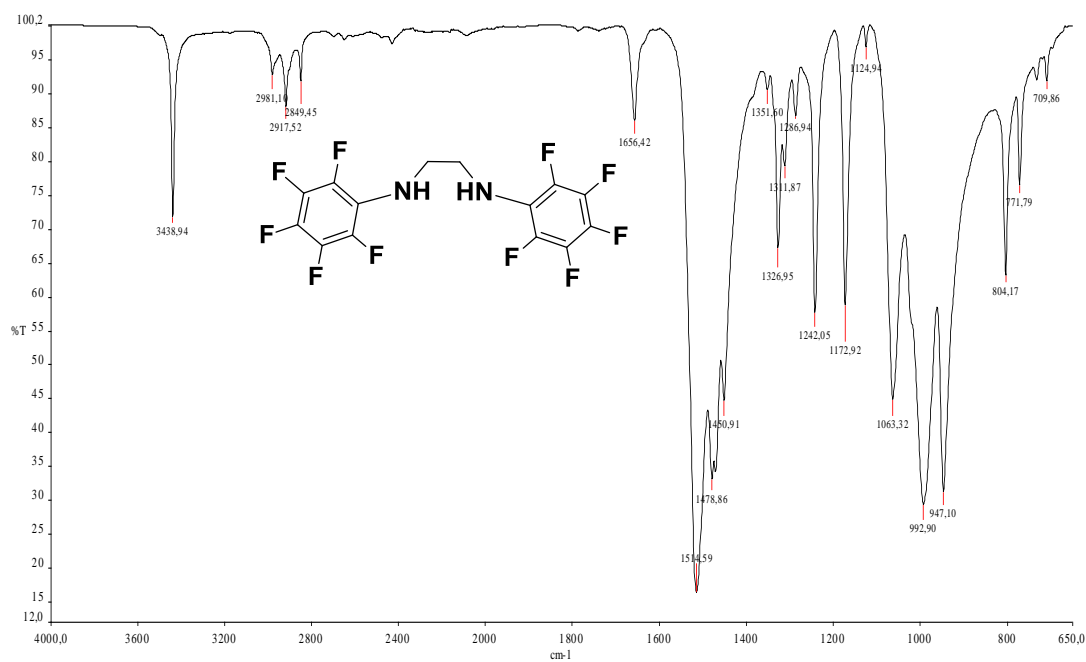
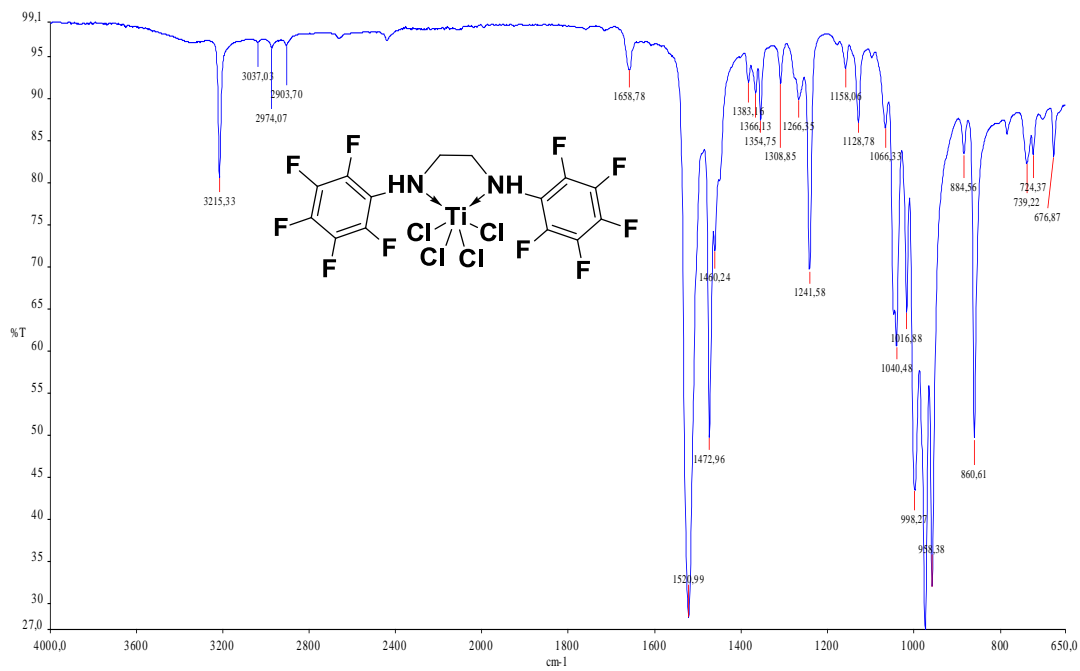
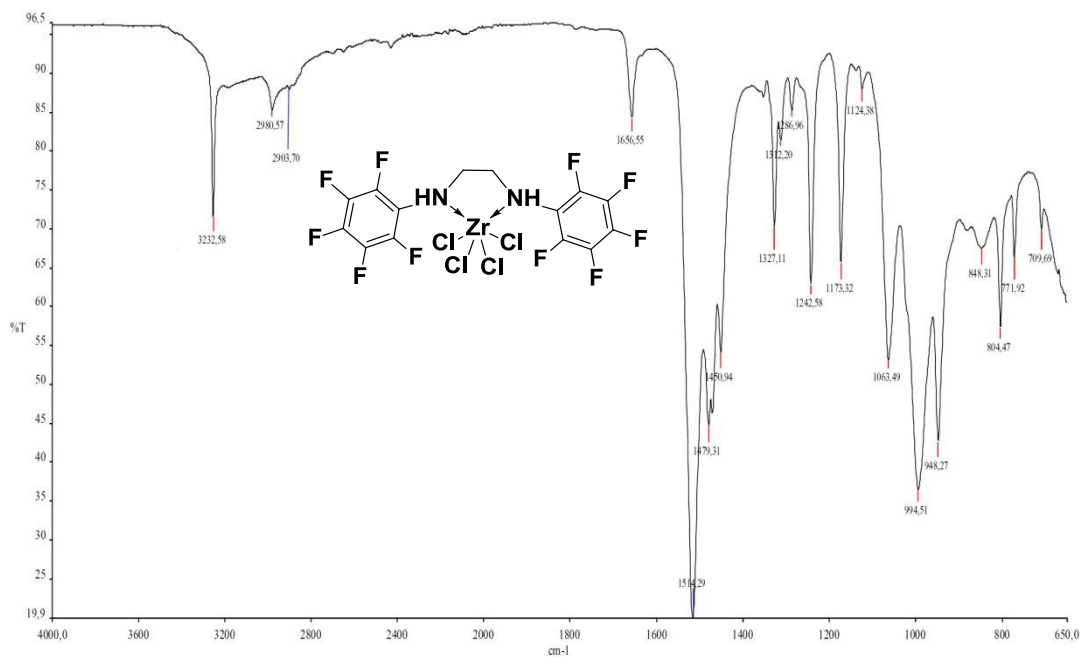


Figure A.21 : FT-IR spectrum of 1.



**Figure A.22 : FT-IR spectrum of 2.**



**Figure A.23 : FT-IR spectrum of 3.**

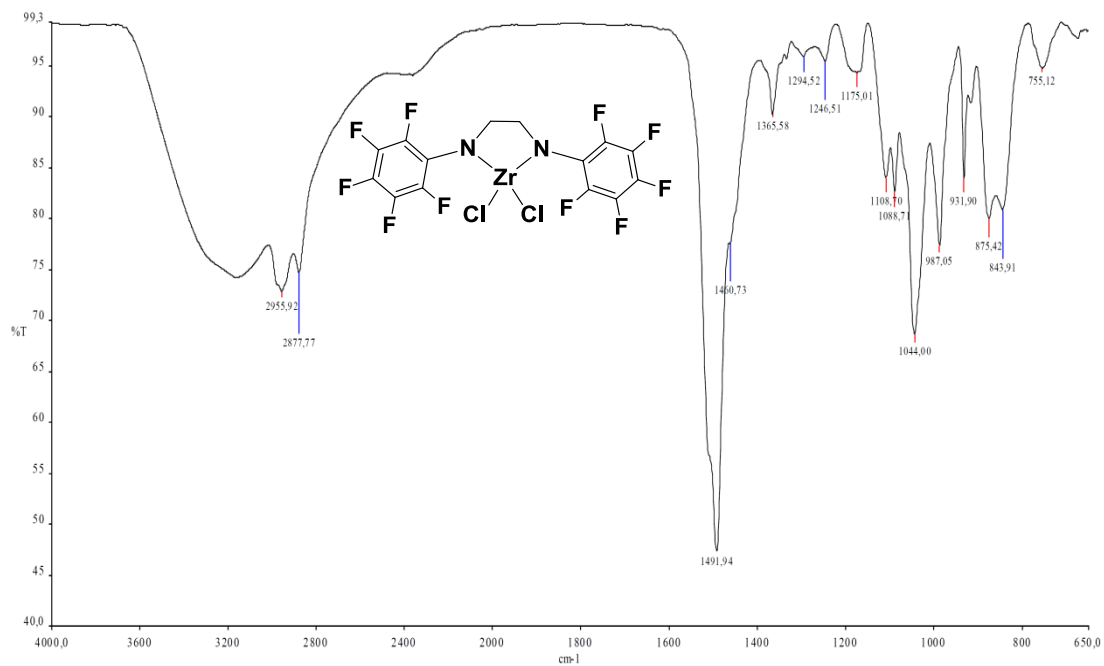


**Figure A.24 : FT-IR spectrum of 6.**

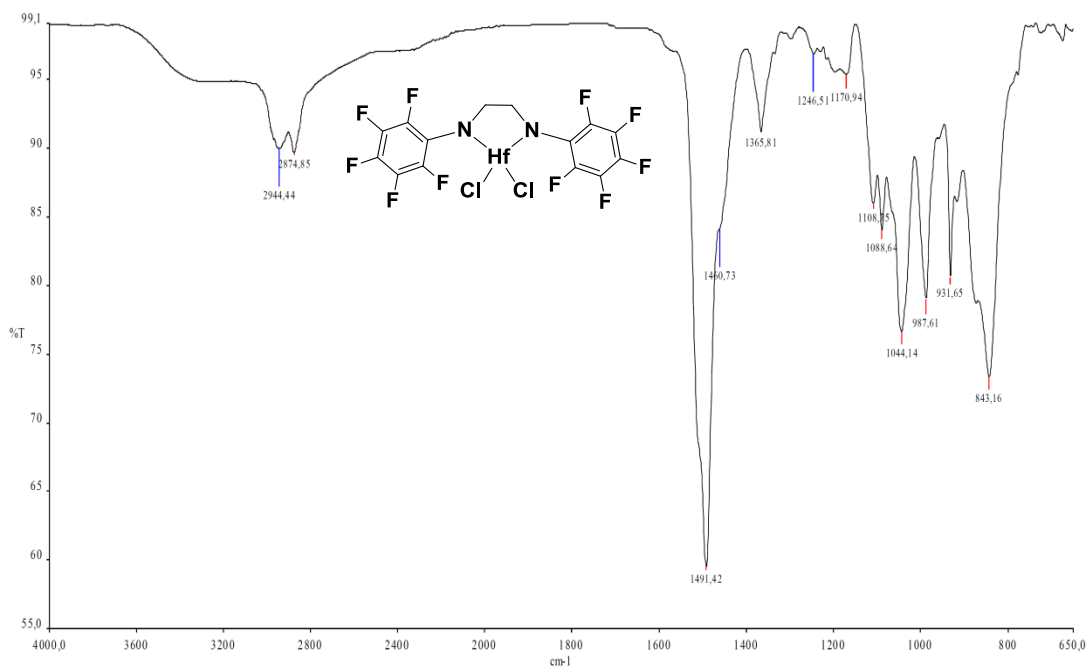


**Figure A.25 : FT-IR spectrum of 7.**



## CURRICULUM VITAE



**Name Surname:** İsmail Hakkı YÜCEL  
**Place and Date of Birth:** İstanbul/ 20.01.1986  
**Address:** İzzetpaşa Mah. Yeniyol Cad. No:6 D:1 Şişli/İstanbul  
**E-Mail:** ismailhyucel@gmail.com  
**B.Sc.:** Ege University Faculty of Science Department of Chemistry

## PUBLICATIONS/PRESENTATIONS ON THE THESIS

- Şentürk, O. S. Yücel, İ. H. ; 2011: Etilendiaminin Titanyum, Zirkonyum, Hafniyum Komplekslerinin Sentezi ve Karakterizasyonu 25. *Ulusal Kimya Kongresi* 28 Haziran-2 Temmuz, 2011 Erzurum, Turkey.